

# Wood Fingerprints

– *Recognition of sawn wood products*



Tobias Pahlberg



Licentiate Thesis

# Wood Fingerprints

Recognition of sawn wood products

**Tobias Pahlberg**



Wood Products Engineering  
Division of Wood Science and Engineering  
Department of Engineering Sciences and Mathematics  
Luleå University of Technology,  
Skellefteå, Sweden

**Supervisors:**

Olle Hagman and Matthew Thurley

Licentiate Thesis  
Department of Engineering Sciences and Mathematics  
Luleå University of Technology,  
Skellefteå, Sweden

This thesis has been prepared using L<sup>A</sup>T<sub>E</sub>X  
All rights reserved  
Copyright © Tobias Pahlberg, 2014.

Wood Products Engineering  
Division of Wood Science and Engineering  
Department of Engineering Sciences and Mathematics  
Luleå University of Technology,  
Skellefteå, Sweden  
SE-931 87 Skellefteå, Sweden  
Phone: +46(0)910 58 5336

Author e-mail: [tobias.pahlberg@ltu.se](mailto:tobias.pahlberg@ltu.se)

Printed by Luleå University of Technology, Graphic Production 2014

ISSN 1402-1757  
ISBN 978-91-7439-909-7 (print)  
ISBN 978-91-7439-910-3 (pdf)

Luleå 2014

[www.ltu.se](http://www.ltu.se)

*I'm leaving my fingerprints*  
*I'm leaving my fingerprints*  
*I'm leaving my fingerprints on you*

*– Katy Perry*



---

---

# ABSTRACT

---

---

This thesis deals with wood fingerprints and presents ways to track sawn wood products through an industrial process using cameras. The possibility to identify individual wood products comes from the biological variation of the trees, where the genetic code, environment and breakdown process creates a unique appearance for every board. This application has much of the same challenges as are found in human biometrics applications.

The vision for the future is to be able to utilize existing imaging sensors in the production line to track individual products through a disordered and diverging product flow. The flow speed in wood industries is usually very high and with a high degree of automation. Wood fingerprints combined with automated inspection makes it possible to tailor subsequent processing steps for each product and can bring the operators vital feedback on process parameters.

The motivation for this work comes from the wood industry wanting to keep track of products without invasive methods such as bar code stickers or painted labels. In the project *Hol-i-Wood Patching Robot*, an automatic scanner- and robot system is being developed, where there is a need to keep track of the shuttering panels that are going to be mended by several automatic robot systems.

In this thesis, two different strategies to recognize previously scanned sawn wood products are presented. The first approach uses feature detectors to find matching features between two images. This approach proved to be robust even when subjected to moderate geometric- and radiometric image distortions. The recognition accuracy reached 100% when matching high quality scans of Scots pine boards that have more than 20 knots.

The second approach uses local knot neighborhood geometry to find point matches between images. The recognition accuracy reached above 99% when matching simulated Scots pine panels with realistically added

noise to the knot positions, whilst more than 85% of the knots were found.

Both presented approaches proved to be viable options for recognition of sawn wood products. In order to improve the recognition methods further, a larger dataset needs to be acquired and a method to calibrate parameter settings needs to be developed.



---

---

# PREFACE

---

---

The work presented in this Licentiate thesis has been carried out at Wood Products Engineering at the department of Engineering Sciences and Mathematics at Luleå University of Technology, Campus Skellefteå. This work has been a part of the *Hol-i-Wood Patching Robot* project which has been financed by the European Union's Seventh Framework Programme (FP7/2007-2013). I am truly thankful for this inspiring project which was the biggest reason why I decided to start my Ph.D. studies in the first place. In this project I want to send a special thanks to a few people at MiCROTEC whom I have had plenty of discussions with; Marco Boschetti, Mauro Cossi and Giovanni Bortolozzo.

Furthermore, I would like to thank my colleges at Wood Products Engineering, Wood Technology, Wood Physics and all the rest at Campus Skellefteå. Thank you for your friendship and support.

Thanks to all of you who have proof read my work and given me valuable feedback, especially Erik Johansson, Anders Berglund and Peter Bomark.

Thanks to my supervisors Olle Hagman and Matthew Thurley. I appreciate your guidance, encouragements and enthusiasm.

Lastly, I would like to thank my loving family and especially my wife Maria.

Skellefteå, April 2014

Tobias Pahlberg



---

---

# LIST OF PUBLICATIONS

---

---

This thesis is based on the following publications:

**Paper I**

T. Pahlberg and O. Hagman, 2012: Feature Recognition and Fingerprint Sensing for Guiding a Wood Patching Robot. In P. Quenneville, Ed., *World Conference on Timber Engineering*, Pages 724–733.

**Paper II**

T. Pahlberg, O. Hagman and M. Thurley, 2014: Recognition of boards using wood fingerprints based on a fusion of feature detection methods. *Submitted to journal*.

**Paper III**

T. Pahlberg, E. Johansson, O. Hagman and M. Thurley, 2014: Wood fingerprint recognition using knot neighborhood  $K$ -plet descriptors, *Submitted to journal*.

## **Contributions to the papers**

In Papers I-II, Pahlberg had the main responsibility for data collection, algorithm development, testing and writing. Guidance and feedback was provided by the co-authors.

In Paper III, Pahlberg and Johansson had equal responsibility in the algorithm development. Pahlberg wrote the main part of sections: Introduction, Related work and Material and methods. Johansson added to the Methods, ran performance tests and wrote the main part of the Results and Discussion sections. Guidance and feedback was provided by Hagman and Thurley.

---

---

# CONTENTS

---

---

<b>Part I</b>	<b>1</b>
CHAPTER 1 – INTRODUCTION	3
1.1 Aim . . . . .	3
1.2 Objectives . . . . .	4
1.3 Limitations . . . . .	4
1.4 Overview of the thesis . . . . .	5
CHAPTER 2 – BACKGROUND	7
2.1 Hol-i-Wood Patching Robot . . . . .	7
2.2 Visual features on timber surfaces . . . . .	8
2.3 Traceability in the forest-wood chain . . . . .	13
2.4 Object recognition . . . . .	15
CHAPTER 3 – MATERIALS AND METHODS	19
3.1 Acquiring of board images . . . . .	19
3.2 Cropped board images . . . . .	20
3.3 Feature detection and matching . . . . .	21
3.4 Removal of erroneous matches . . . . .	24
3.5 Simulated panel images . . . . .	25
3.6 Creating test datasets . . . . .	26
3.7 Neighborhood descriptors ( $K$ -plets) . . . . .	27
CHAPTER 4 – RESULTS AND DISCUSSION	29
4.1 Geometric distortions . . . . .	29
4.2 Improvements . . . . .	31
4.3 Matching smaller image pieces . . . . .	33
4.4 Matching panels using $K$ -plets . . . . .	34
CHAPTER 5 – CONCLUSIONS	37
CHAPTER 6 – FUTURE WORK	39

REFERENCES	41
<b>Part II</b>	<b>47</b>
PAPER I	49
PAPER II	61
PAPER III	77

# Part I





---

---

# CHAPTER 1

---

---

## Introduction

Why would we need a “wood fingerprint”? Identification of humans is a need which is easier to understand. We are in need of security and the possibility to prove ownership of certain property.

The wood fingerprint is a tool that can be used to keep track of individual wood products throughout a production chain. In today’s global economy there is a constant battle for sawmills and other wood industries to increase the efficiency of their production, to survive in the tough competition. Tracking opens up the possibility to individualize the processing of each product, monitor the processes and adjust machine settings in real-time.

Wood fingerprint research lies in between the areas of Computer vision, Wood technology and Biometrics. Wood technology and biometrics are by themselves large research areas and they both utilize computer vision in many ways. However, for some reason, not much technology transfer has yet occurred between wood technology and biometrics. Hence, wood fingerprint recognition is an underexplored and open field.

### 1.1 Aim

The aim of this Licentiate thesis is to give an introduction to fingerprint recognition of sawn wood products and to present two possible approaches to the problem. The aim in Papers I-III has been to develop and evaluate methods for recognition of previously scanned wood products. Our

goal has been to reach as high recognition rate as possible while using a database of hundreds of individuals.

The approach has been to draw inspiration from computer vision and human biometrics and to utilize general and robust methods to maximize the applicability. Our goal is that the results presented here will give the industry an idea of the possibilities and performance of wood product recognition, and that we will inspire to more research in the field.

## 1.2 Objectives

Paper I:

- Develop a framework for matching wooden boards against a closed set of images, where the sought board is known to be in the database.
- Evaluate the robustness of the chosen approach with respect to realistic geometric and radiometric distortions.

Paper II:

- Improve the matching performance from Paper I.
- Investigate how the number of knots on a board relate to the recognition accuracy.

Paper III:

- Develop a recognition method based on geometric relationships between knots.
- Evaluate the performance on wooden panels.

## 1.3 Limitations

The material used in this thesis consists of boards from Scots pine (*Pinus Sylvestris* L.) grown in central Sweden. This is a material with a quite regular knot frequency and our main focus has been to detect and utilize the knots as a recognizable signature. Without knots on the wood surfaces, the presented methods will not perform very well.

While there are many ways to image wood, e.g., using laser, multispectral imaging and X-ray, we have only utilized grayscale image information from the visible spectrum for recognition.

## 1.4 Overview of the thesis

Chapter 2 aims to give the reader a basic introduction to the Hol-i-Wood Patching Robot project, common features on timber surfaces, traceability in the forest-wood chain and object recognition. Chapters 3-4 includes a condensed version of the materials, methods, results and discussion of the appended papers. In Chapter 5-6, conclusions are stated and possible future work is discussed.

Part II of this thesis consists of the three papers in their entirety. Figure 1.1 gives a quick visual summary of the ideas and questions that preceded the papers, and their respective outcomes.

Paper I was inspired by multi-view image registration, where often so called *feature detectors* are used to find matching points between images. A survey was conducted on literature concerning object detection and different feature detectors. This paper is focused on recognition of full-length floorboards under the influence of both geometric and radiometric image distortions.

Paper II was focused on improving on the results and shortcomings of Paper I. The parameters of the previously used feature detectors were altered and the two methods were this time combined. The improved methods were tested both on full-length boards, but also on smaller wood pieces. The aim was to investigate how the recognition performance was connected to the number of knots on the boards.

In Paper III, an entirely different approach was pursued, inspired by a method sometimes used within fingerprint- and face recognition. The idea was to calculate distances and angles between meaningful points on wooden panels, in our case, the knots.

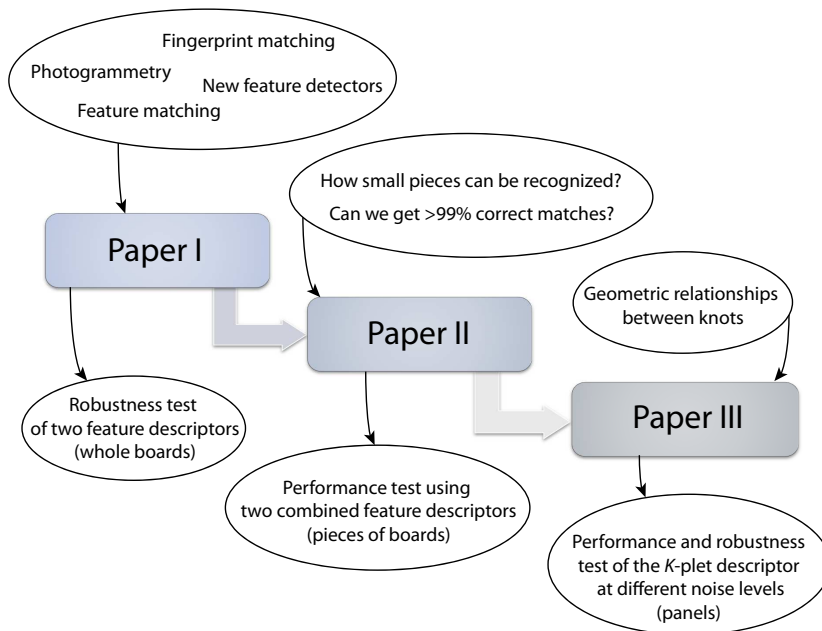


Figure 1.1: Overview of papers. Ideas/questions on the top and outcome on the bottom.

---

---

# CHAPTER 2

---

---

## Background

### 2.1 Hol-i-Wood Patching Robot

The European Union's FP7-project *Hol-i-Wood Patching Robot* has been the platform on which the research presented in this thesis has been conducted.

Today, about 20 people work in shifts in the process of repairing defects on wood products such as laminated beams and shuttering panels at the Slovenian company LIP-BLED. The goal of this project is to develop a commercial patching robot system which is able to reduce production costs for the wood products and also to obtain a more consistent product quality. With the system, only a couple of people should be required to carry out the same job.

The prototype patching plant will be assembled at LIP-BLED and tested on their three-ply panels which are used as formwork for molding concrete in the construction industry.

Using a state-of-the-art wood scanner, the panel is first illuminated with LED and laser lights and the defects and their positions are stored. At the same time, the fingerprint is extracted. The panel is then passed on to any of the (at least) six robot stations where another camera recognizes the fingerprint. The defects that were meant to be patched are repaired automatically while other cameras at the robot help to position the panel. The defects are drilled out and wooden dowels are pressed down in the

hole. The entire process takes no more than two seconds per patch.

One of the most challenging and innovative ideas in this project has been to develop a system for recognizing the wood panels using just their own fingerprint. This approach would remove the need for invasive tracing methods, such as bar code stickers or painted labels.

The database of products in which to search, consists of the panels which have been scanned and are on their way to a patching robot. The size of the database will affect both the possibilities to find a correct match and the time it takes to do the re-identification.

## 2.2 Visual features on timber surfaces

Wood is a biological material. Every stem, log and board has its unique individual properties because every tree has its own genetic code (Kvarnström and Oja, 2010). Moreover, trees are reacting to different climates, seasons and other external influences. Trees turn out different depending on if the soil is nutritious, if the soil has an adequate moisture level or if there is a good amount of sunlight (Bijak, 2007).

In this section, a few of the most common features on timber surfaces are explained, see Figure 2.1. A lot of research has been carried out to improve automatic detection of these features. However, there is a lack of research concerning how to recognize for example a specific knot or crack. Keep in mind that there is a difference between detection/classification and recognition, and that this explains why there may be differences in the approaches to these problems.

### 2.2.1 Growth rings

Trees add new layers of cells just under the bark in an outward direction (Panshin and De Zeeuw, 1970, p. 16). The *growth rings* in trees become visible due to different weather conditions during the year, where the cells produced in winter have thicker walls. Trees in temperate forests usually add one visible ring each year. They are therefore often referred to as *annual rings*.

Most work on growth ring detection has been done on log ends (Cerdeira et al., 2007; Norell, 2011).

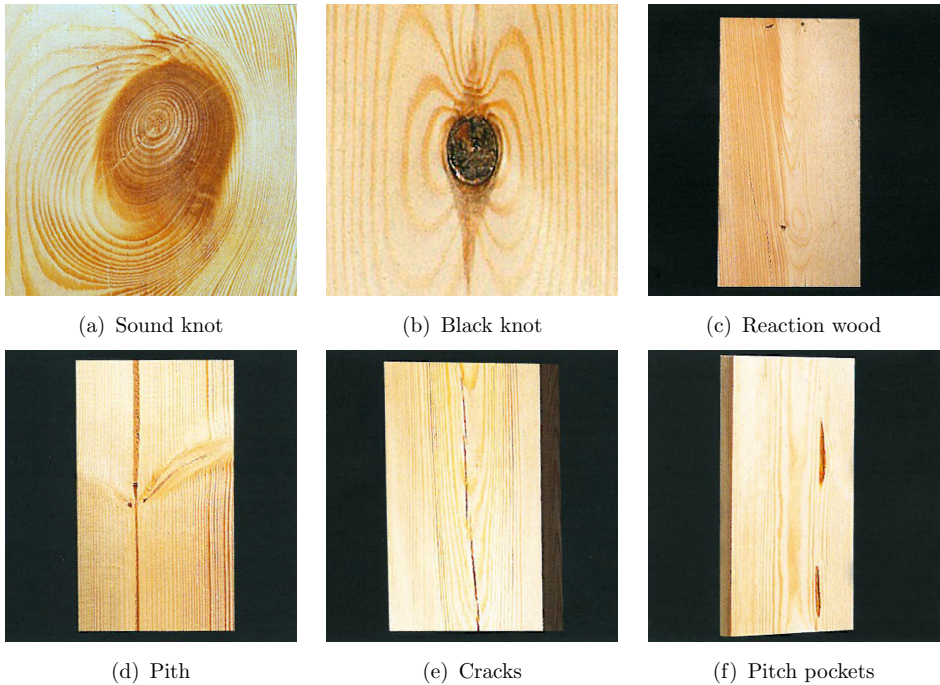


Figure 2.1: Examples of a few common visual features on timber surfaces. (Illustrations from Anon (1997))

### 2.2.2 Knots and knot types

Branches on trees are formed in the same way that the main tree stem is formed (Wangaard, 1981, p. 110). The branches propagate into the stem and are in there referred to as *knots*. The knot can be either dead or alive. If the cambium<sup>1</sup> is still alive at the point where the branch fuses with the stem, then the knot is alive, also called *green* or *sound* knot (Dinwoodie, 1981, pp. 4-5). However, if the cambium around the branch is dead, it is called a *dead* or *black* knot. Often, trees self-prune themselves, felling their lower branches. These dead knots are after a while overgrown by the trunk, and during sawing, they will often loosen and fall out.

Depending on the direction in which the log is cut, knots will appear in different ways, most often some sort of ellipse.

Knots are often the most salient, distinct, feature on planks and boards.

<sup>1</sup>The cambium is a thin layer just underneath the bark where new wood cells are produced.

When grading timber for appearance, the most important factors are: type of knots, distribution of knots, size of knots and coloration of the timber (Lycken, 2006, p. 6). Hence, knots are likely the most important visual information that also can be utilized by a computer for recognition purposes.

Knot detection can be carried out directly in color/grayscale images (Funck et al., 2003; Todoroki et al., 2010), using the tracheid effect<sup>2</sup> (Åstrand, 1996, p. 59) or in X-ray images (Longuetaud et al., 2012; Johansson et al., 2013).

### 2.2.3 Heartwood and sapwood

Most trees form *heartwood* in the inner part of the trunk during its lifetime. Heartwood formation is a result of a naturally occurring chemical transformation which makes that part of the tree more resistant to decay (Capon, 2005, p. 65). The transport of free water stops between cells in the heartwood and the living cells die. Hence, the water transport from the bottom to top of the tree is only performed by the outer part of the stem, the *sapwood*.

Visually, the heartwood usually appears somewhat darker than the sapwood, this is due to the various extractives which are present (Ek et al., 2009, p. 26). However, high water content will also lead to a deeper light penetration, often giving moist wood a darker tint (Birth, 1978; Hagman, 1996). Some trees do not form discolored heartwood, these trees are referred to as sapwood trees (Wangaard, 1981, p. 110).

Heartwood border was detected on log ends by Gjerdrum and Hib (2004) using infrared imaging. Skog and Oja (2010) successfully measured heartwood diameter in logs using a combination of X-ray and 3D-data.

### 2.2.4 Reaction wood

Reaction wood is formed under load or stress induced by gravity or wind pulling and pushing the tree sideways. The purpose of reaction wood is to try to keep the tree in an upright position (Ek et al., 2009, p. 66). It is always present in branches that are directed non-vertically and therefore

---

<sup>2</sup>When a wood surface is illuminated by a concentrated light source, e.g., a laser, the light will mainly spread along the wood fibers, called tracheids in softwood, giving an elliptical spot.



always subjected to the gravitational force. The cells in reaction wood differ both in cell wall structure and in the content of substances compared to the regular cells. These differences give them a slightly different color.

Reaction wood was successfully detected by Nyström and Hagman (1999b) and Duncker and Spiecker (2009) in multispectral images. Nyström and Hagman (1999a) evaluated the detection of reaction wood using color scanning, tracheid effect and X-ray scanning.

### 2.2.5 Pith

The pith follows the center of the stem. It represents the tissues formed during the first year of growth for each level of the stem (Ek et al., 2009, p. 26). The top part of the tree will form the pith as the tree grows. It will usually show up as a dark stripe on the surfaces of center boards, running in the stems lengthwise direction. Detection of pith has mostly been done in CT images and on log ends (Norell and Borgefors, 2008; Boukadida et al., 2012).

### 2.2.6 Cracks (checks and splits)

Cracks in wood can form by several different reasons. According to Lamb (1992), they can be caused by growth stresses or environmental conditions. Processing cracks are caused during machining or kiln drying. They can also appear at a later stage by shrinking and swelling when the moisture content of the wood is different from its surroundings. Cracks can also form due to mechanical damage and faulty design.

In color images, cracks can often be misclassified as pith, and vice versa, due to the similarities in shape. However, most modern wood scanners often include some sort of depth measuring approach to detect cracks (WoodEye, 2014; GoldenEye, 2014).

Patricio et al. (2005) detected very thin cracks in intensity images of pallets using frequency histograms of connected elements and an artificial neural network classifier.

### 2.2.7 Pitch pockets

Pitch-, or resin pockets, consists of an opening in the grain that contains, or at least at some point has contained pitch (resin). Pitch pockets are found in softwoods in which resin canals are normal in the wood. Pitch pockets are most common in small to medium sized trees growing on windy sites where the cambium is subject to considerable flexure (Walker, 2006, p. 8).

Pitch pockets on timber surfaces can often be found using color images since the pitch is usually yellow (Lampinen et al., 1994). Pitch pockets were detected in color images and classified using a neural network by Estevez et al. (2003). UV light in combination with a color sensor showed good possibilities to detect pitch pockets on open wood surfaces in Hagman and Nyström (2003).

## 2.3 Traceability in the forest-wood chain

Traceability is the ability to track a product or a product batch and its history through a production chain (Moe, 1998). Well thought-out traceability systems are fundamental for achieving optimal benefits from quality control, production control and for fulfilling consumer demands. A system transmitting information about products through the supply chain can significantly reduce operating costs and can increase productivity by increased control over production (Regattieri et al., 2007).

The forest-wood chain is a so called *continuous process*. Continuous production processes schedule long production runs where setups are seldom changed and the production flow is organized in a certain sequence (Kvarnström and Oja, 2010). The products in continuous processes usually undergo many different stages or phases and the products are often mixed, reshaped or transformed.

Traceability has long since been an important topic within chemistry, medicine, food and manufacturing of vehicles (Taverniers et al., 2004; Hobbs et al., 2005; Sohal, 1997). The food industry might be one of the most similar areas to the wood industry concerning traceability, since they also have to deal with the diversity of biological materials.

In the sawmill industry the raw material costs account for 65-75% of the total production cost for modern sawmills (Wood Resources International, 2013). Therefore, any small change that can improve the way the material is utilized has a big economical impact.

In the forest industry an important decision is already being made when the harvester fells a tree and decides where to cross-cut (buck) the stem into logs (Kvarnström and Oja, 2010).

Simplified, the different stages between forest and sawn lumber can be summarized as follows:

1. **Harvesting**, the tree is felled and the branches are cut away. The stem is then automatically bucked at a certain positions depending mainly on diameter and a price list for different product lengths.
2. **Log sorting**, the logs are presorted into different bins according to top diameter, quality and length.
3. **Batch sawing**, the logs are sawn into planks and boards.

4. **Green sorting**, the planks and boards are sorted into different bins according to thickness, width and sometimes grade, depending on customer demands.
5. **Drying**, the planks and boards are put into large drying kilns to lower their moisture content under controlled forms to later prevent geometric distortions and crack formation.
6. **Planing**, the planks and boards are planed to meet different quality standards of different product classes. The goal is to maximize product value.
7. **Final sorting**, the finished products are sorted by grade and/or length and packaged.

Through all of the above mentioned steps and throughout secondary processing there are benefits to tracking the wood. There are many reasons why:

- *To obtain instant feedback on product quality.* In modern factories the production speed is usually very high, often too high for humans to realize if something is wrong. In modern sawmills for example, the process speed lies at about two meters per second. The speed in combination with a high degree of automation means that if a machine is badly calibrated one can lose money fast. Sometimes, certain defects are not even discovered until after the shipping to customers. Then the products might need to be recalled, which can be very expensive (Jacobs, 1996). Traceability is a tool for keeping a more consistent quality of the products.
- *To be able to tailor the production process and the produced products to suit different customers.* Different customers have different specific preferences concerning dimensional tolerances, visual appearance and strength. The profit can be increased if the choice of log can be tailored to a specific product and customer.
- *To be able to certify the origin of the wood.* Traceability makes it possible to for example prove that a product is based on wood from a forest which is managed in a sustainable way (Kvarnström and Oja, 2010).

- *To be able to trace good or bad raw material properties back to its origin.* Traceability makes it possible to market and promote a special raw material or certain product features (Moe, 1998). It will also be easier to separate high- and low quality raw materials if desired. If rot, diseases or insect infestations are discovered at late stages, there is a possibility to quickly detect and map the spread of the problem, identify a possible cause and take actions.
- *To reduce the number of measuring instruments and to remove unnecessary repetition of measurements.* In sawmills today, measurement information is often collected at one stage and then discarded, even though it might be useful at a later stage.

Large efforts have been made to introduce a tracing system of trees already in the forest using *radio-frequency identification* (RFID) tags (Uusijärvi, 2000; Kvarnström and Oja, 2010). But in continuous processes there is seldom a single method that can be used to track the products throughout the whole chain.

According to Kvarnström and Oja (2010) there are a few suitable methods for on-line tracking of wood products:

- *Process data.* In some continuous processes there are changes in the raw material properties which can be measured and used for tracking.
- *Material signature (fingerprint).* Just like humans have unique fingerprints, similar highly unique properties might be found in the structure of a material.
- *Traceable marker (or unit).* Marking techniques such as barcode stickers, painted codes, magnetic stripe cards and RFID tags are sometimes used.

## 2.4 Object recognition

How can we make a computer recognize something? The biometrics and computer vision field has solved many of these problems before, and often the methods are tailor-made to recognize for example a certain shape or a collection of attributes. These methods often require us to teach a



Figure 2.2: To separate and recognize objects is an easy task for humans. Here are two examples which are not so trivial for a computer. (a) Different grayscale textures. (b) Some random objects on my desk.

classification program what is right and wrong, set up rules. But how can we make a computer recognize something without a special shape? When mass producing standardized products, like in the wood industry, there can be thousands of products with almost exactly the same outer dimensions. We can get ideas for solutions by trying to mimic what humans do to recognize objects. Our eyes and brain are trained at recognizing objects from the day we are born, and it is usually very difficult to build an artificial classifier that outperforms a human (Russell and Norvig, 2003, Chap. 24).

Visually, humans react to high contrast changes, contours, shading and texture changes. We can quickly see boundaries of objects and can compare geometric relationships between things that we see, with or without occlusion. Try looking at the examples in Figure 2.2. To distinguish between these different areas and objects is not trivial for a computer.

A good place to start can be a computer program which reacts to salient features in an image. Texture patterns can often be used to classify materials, but it can be difficult to separate specific individuals using this technique.

In object recognition tasks, there are usually a few design challenges which need to be dealt with:

1. How to acquire and pre-process the input images?
2. How to describe and represent object features using a computer?

### 3. How to match these features?

Often the solution can involve detection of *interest points* in an image and the extraction of some regional information around these interest points (Belongie et al., 2002; Lowe, 2004; Bay et al., 2008).

#### 2.4.1 Recognizing sawn wood surfaces

There are many approaches one can use to recognize sawn wood products. Every feature on the wood surface can be utilized. Below are some examples for the two most common features:

##### 1. Knots

- (a) Measures of the knots can be used, e.g., width, orientation, area or average brightness.
- (b) The knots can be classified as for example large black knot, small bright knot, thin knot, round knot. The number of knots in each class and the position of these knots can be used as information for recognition. The distribution of knots and knot types often determines the quality of the boards (Anon, 1997). The quality can in its turn be used as a discriminating factor.
- (c) The x- and y-positions of the knots can be used directly or can be used to calculate distances and angles between knots.
- (d) The intensity values in an area around the knots, or a lower dimensional representation of these values, can be stored.

##### 2. Growth rings and texture

- (a) Growth rings can be used similar to a bar code. The distances between them and the thickness of them can be used.
- (b) Interesting positions along the growth rings can be stored, e.g., where the lines change direction quickly.
- (c) The texture can be classified for different regions and be utilized.





---

---

# CHAPTER 3

---

---

## Materials and methods

In all three appended papers, the same raw material has been utilized. This dataset consists of 886 floorboards of Scots pine (*Pinus sylvestris* L.). The cross-sectional dimensions of the boards are 21x137 mm and they are between 3007-5109 mm long. An example of a few boards can be seen in Figure 3.1. The boards were sawn from 222 logs with top diameter between 201-215 mm which were randomly collected from Bollsta sawmill in central Sweden. They were then planed, sanded and finished with white pigmented oil and a thin layer of varnish.

### 3.1 Acquiring of board images

The finished floorboards were originally scanned for a customer preference study in 2006 (Nyström et al., 2008; Broman et al., 2008; Oja et al., 2008). The images were acquired using a high resolution color line scan camera; Dalsa Trillium TR-37. The image colors and contrast was carefully calibrated and 8 cm were cut off each end of the images to prevent edge artifacts. Lastly, the images were downsampled to a resolution of 1 pixel/mm in both dimensions.

A second set of images was produced by Pahlberg and Hagman (2012) by adding different levels of scaling, rotation and skewing to a subset of the original images. See an example in Figure 3.2(b).

A third set of images was acquired using the same line scan camera as before, where 44 random floorboards (5%) were re-scanned. The scan

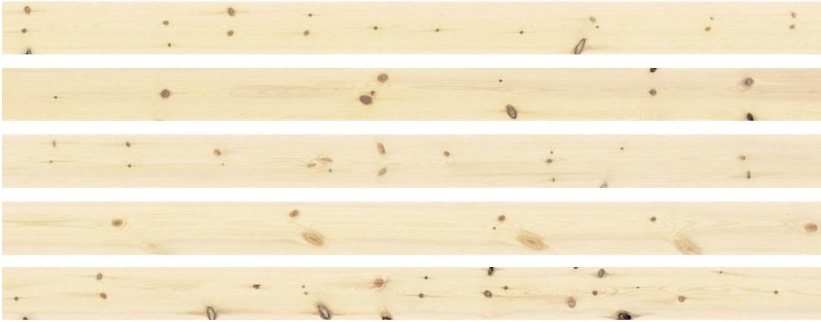


*Figure 3.1: Example of a few boards from the original floorboard dataset.*

was done to obtain a realistic second version of images that could be used when testing recognition algorithms. Some of the boards had during the past years of storage become somewhat crooked or bowed. Moreover, this time no stabilization of the boards was carried out while the conveyor belt was transporting them past the camera. No color corrections were made on the images and some dust stains were present on a few floorboards. Furthermore, this time the edges of the board images were not cut off, making them 8 cm longer on each side.

These new images were of high quality but otherwise differed quite much in appearance, see an example in Figure 3.2(c).

Lower quality digital photos were also taken of the floorboards from a distance to provide a tougher challenge for the recognition methods, see Figure 3.2(d). These photos were acquired with a Canon 400D camera. The re-scanned images were downsampled and the Canon photos upsampled to 1 pixel/mm.

## 3.2 Cropped board images

In Paper II, several sub-datasets were created from the re-scanned images and the digital photos. The knots were manually marked in the images and from that information the board images were cropped at different positions so that all board pieces in one subset would have the same amount of knots (Figure 3.3). The cropped datasets were created to investigate how many knots, on average, was needed to obtain a certain matching accuracy.

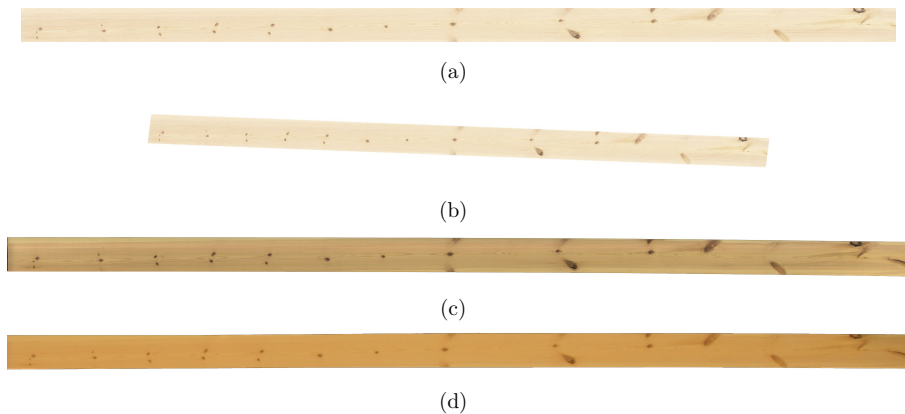


Figure 3.2: (a) Original images scanned 2006. (b) An example of a geometrically distorted version of the same board image. (c) The same re-scanned board (black borders have been removed here). (d) A digital photo of the same board taken with a Canon 400D (black borders have been removed here).

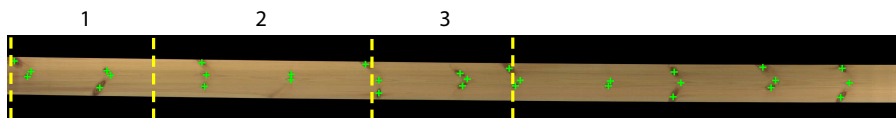


Figure 3.3: The crop positions were automatically placed in between knots after they had been manually marked. In this example, board pieces with six knots are extracted. A maximum of three pieces were grabbed from each full length board.

The results would give an idea of how well these methods would work for a material input with fewer knots. A close-up of a wood piece with five knots can be seen in Figures 3.4(a)-(c). Here, a cropped version of the original image is shown as reference, but the Canon and Re-scanned cropped images were always matched against full-length original boards.

### 3.3 Feature detection and matching

In Paper I and II feature detectors are used to solve the closed-set recognition task, where the sought individual product is known to be in the database. Two different feature detectors which extract local brightness information around interest points were investigated. Interest points are

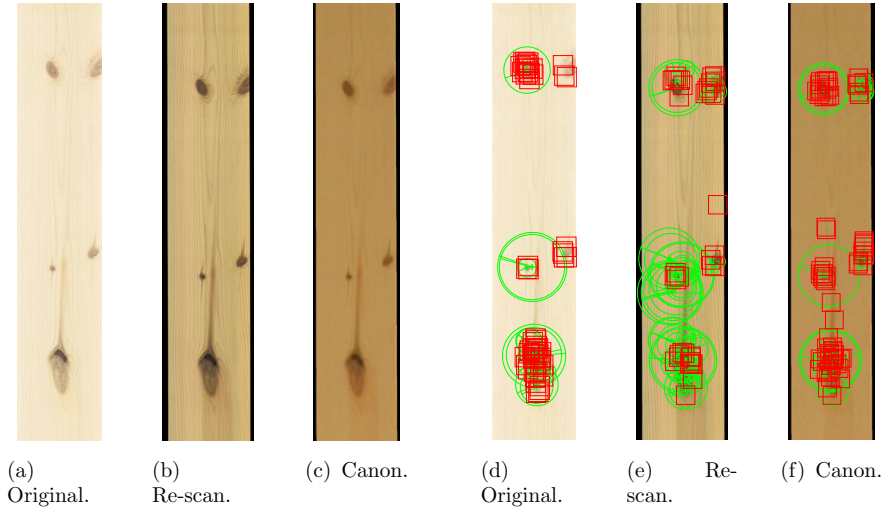


Figure 3.4: Examples of the cropped datasets with an approximate number of knots per image. Image (a) is shown as a reference to (b) and (c) which are part of the 5-knot batch. Figures (d)-(f) are the same images but now showing where the Block and SURF features are detected. Block features are marked by red squares and SURF features by green circles.

regions in an image that are likely to be recognized in other images of the same scene or object. Typical interest points include, for example, corners, line endings and blobs (Schmid et al., 2000). On sawn wood surfaces, blob- and corner detectors usually find most interest points in the middle or around the knots.

An example of how the two different methods place their feature descriptors, can be seen in Figure 3.4(d)-(f).

In Paper I and II, the procedure for finding a best matching wood piece in the database can roughly be described as follows:

1. Load a query image.
2. Invoke a corner/blob detector on the image and extract feature descriptors around those corners/blobs.
3. Remove feature descriptors that are partly outside of the wood piece border.

4. Match the query board descriptors against the descriptors of the database boards, one board at a time by calculating the sum of squared differences (SSD) between them.
5. Estimate a best fitting geometric transformation between point matches. Remove outlier matches that don't fit the transformation and evaluate if the transformation seems reasonable in terms of rotation and scale.

When matching a piece of wood against a database of images, the best database hit to a query image is the one that gets the most matching feature points. A certainty measure of the correctness of this match can be obtained by comparing with the second best hit's number of matching feature points. If the best matching board has many matching features and the second best match has significantly fewer, then we can be quite certain that we have a correct match.

### 3.3.1 Block features

The first type of descriptor is a very basic one, it stores the normalized intensity information in a  $25 \times 25$  square region around each corner, Figure 3.5(a). This block size was chosen as a compromise between a large enough size to encircle substantial parts of most knots, and a not too large size as to result in slow computation times. Relatively small block sizes also makes it possible to extract features close to board edges, where knots quite often are found. Blocks which get positioned partly outside the board edges are naturally discarded.

In Paper I, the *Features from Accelerated Segment Test* (FAST) corner detector was used to find interest points (Rosten and Drummond, 2006). This corner detector was chosen since it seemed to perform well, and at the same time much faster than for example the classical *Harris corner detector* (Harris and Stephens, 1988). However, the results from Paper I showed a weakness of the FAST corner detector. Hence, in Paper II, the more robust Harris corner detector was used instead.

### 3.3.2 SURF features

The second descriptor is called *Speeded-up Robust Features*, (SURF, (Bay et al., 2008)). SURF uses a blob detector to detect features at different

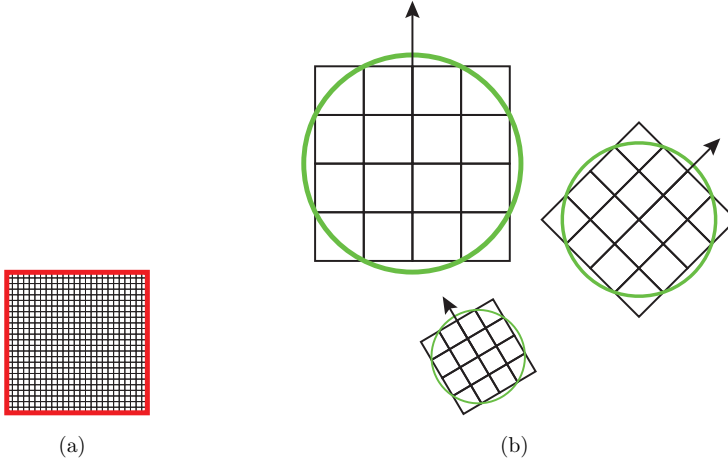


Figure 3.5: (a) A simple  $25 \times 25$  Block feature. (b) Three SURF features which are scale- and rotationally invariant. The dominant direction of the interest points are marked by the arrows.

scales. It stores 64 values containing normalized gradient statistics around each blob, describing the gradient direction and magnitude of 16 sample points. The descriptors are rotated to align with the dominant directions of the blobs, Figure 3.5(b). SURF features allow for the possibility to match descriptors in images of the same object with different scales and rotations. The descriptor regions were set to cover between  $9 \times 9$  mm up to  $147 \times 147$  mm.

For the SURF method, the blob acceptance threshold was lowered in Paper II in order to generate more feature descriptors. The same test was carried out on the updated versions of the two methods. As an additional test in Paper II, the two different feature descriptors were also used in combination.

### 3.4 Removal of erroneous matches

After a feature detection and matching algorithm has done its job, there are usually many falsely matched points. This abundance is by design, since too many true matches otherwise might be removed as a result of image distortions.

In Paper I-III, the number of false matches is reduced by only allowing

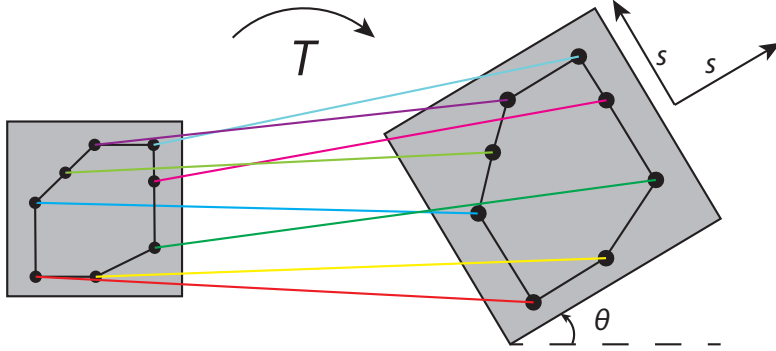


Figure 3.6: The similarity transformation,  $T$ , where  $\theta$  is the rotation and  $s$  is an isotropic scale factor.

point matches that roughly fit a *similarity transformation*. A similarity transformation allows isotropic scaling, rotation and translation. An example can be seen in Figure 3.6. A more thorough explanation can be found in Papers I-II.

### 3.5 Simulated panel images

In Paper III, simulated panel images were created by stitching together four and four randomly picked floorboards from the original dataset (the same original dataset as in Paper I and II). This resulted in a total of 212 unique panel images of size  $3000 \times 548$  mm. The dimensions were chosen, as they were, to be as similar as possible to the formwork panels produced by the industrial partner, LIP-BLED, in the Hol-i-Wood PR project. However, the only information utilized in Paper III was the knot positions. These  $(x, y)$ -positions on each panel were obtained by a semi-automatic approach, where a human would accept or reject the automatically extracted knot positions. First, an automatic segmentation of knots was carried out, then the segmented image was shown on screen for evaluation, as seen in Figure 3.7. A few boards were discarded in this step due to unsatisfying thresholding and bad knot segmentation. However, the aim in this paper was not to develop a perfect knot detection algorithm. This knot detection algorithm was only developed as an aid in the data

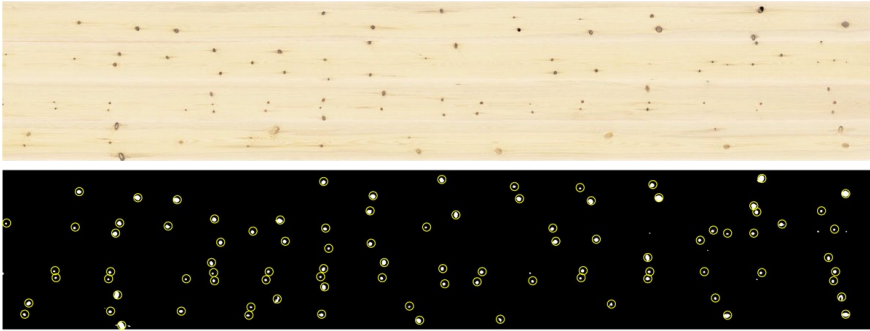


Figure 3.7: On top, a simulated floorboard panel created by stitching together four floorboards and cutting off their lengths at 3000 mm. The lower image shows the thresholded version of the same panel, where the segmented knots have been marked by yellow circles.

acquisition. A high precision of these original knot positions were also not very important for our purpose. The important thing here was to obtain a reasonably sized database of wooden panels with a realistic distribution of knot positions.

### 3.6 Creating test datasets

The recognition method in Paper III depends on knot positions and therefore also on how precise and robust a knot detection algorithm can perform. To simulate a realistic knot detection algorithm, three different noise levels were added to the original knot positions. That is, normally distributed errors with zero mean and standard deviation levels  $\sigma_\epsilon = [5, 8, 11]$  mm. This gave us three query datasets,  $Q_5, Q_8$  and  $Q_{11}$ . Then, 12 different other datasets,  $D_{\sigma,p}$ , were created adding the same error levels in knot positions, but also with a percentage of knots removed on each panel,  $p_\epsilon = [0, 5, 10, 15]$  %.

A schematic overview of the different datasets can be seen in Figure 3.8. For example, query dataset  $Q_5$  was matched to each of the four databases  $\{D_{5,0}, D_{5,5}, D_{5,10}, D_{5,15}\}$ . The matching accuracy was calculated as the percentage of correctly matched panels.



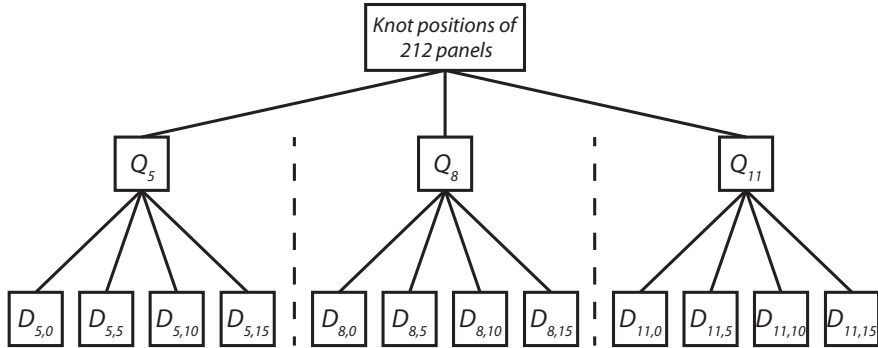


Figure 3.8: Schematic overview of the knot datasets created for the evaluation of the  $K$ -plet recognition method. The  $Q_\sigma$  datasets include the 212 panels with added noise to the knot positions and are matched against the 212 panels in each of the  $D_{\sigma,p}$  datasets, which have both noise added to knot positions and a percentage,  $p$ , of the knots removed.

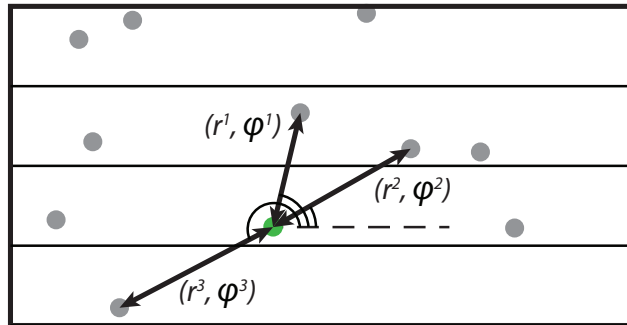


Figure 3.9: The neighborhood descriptor for  $K = 3$  visualised on a surface with gray circles representing neighboring knots. Each of the  $K$  neighbors have a distance  $r^j$  at an angle  $\varphi^j$  to the center knot.

### 3.7 Neighborhood descriptors ( $K$ -plets)

In Paper III, for every knot, a descriptor is created out of the distances and angles to its  $K$  closest neighboring knots, hence the name  $K$ -plet, see Figure 3.9.

The descriptors are then made scale- and rotationally invariant by computing ratios between radial distances and differences between angles.

All  $K$ -plets are then stored as rows in a matrix for each panel.

In order for each  $K$ -plet component to have the same weight in the identification, the distance ratios and angles are also normalized within each panel.

When matching one panel against another, all  $K$ -plets on one panel are compared against all  $K$ -plets on the other panel. The  $K$ -plet-pairs which have a certain dissimilarity level,  $\lambda$ , are removed, the others are kept as potentially correct matches. The dissimilarity between two  $K$ -plets is calculated as the sum of squared differences (SSD). A perfect match will have an SSD of 0, while a bad match will have a relatively high SSD

Several tests were conducted to obtain the optimal  $\lambda$  and the optimal number of knot neighbors,  $K$ .

---

---

# CHAPTER 4

---

---

## Results and discussion

### 4.1 Geometric distortions

In Paper I, the first test was created to evaluate the robustness of the methods towards geometric image distortions.

An example of a successful identification for the two methods can be seen in Figure 4.1.

The results from Paper I show that the SURF method do not handle geometric distortions as well as the Block matching method with the settings used. The biggest difference appears when anisotropic scaling is applied to the image, i.e., when an image is scaled more in one direction than the other. For example, when the images were scaled down 30% in one dimension and 10% in the other, the SURF method gets between 30-50% correct identifications. For the same case the Block matching method lies between 70-100%. However, when the scaling is isotropic, both methods perform quite well. For instance, a 30% size reduction of both length and width, and a 15 degree rotation, yields a recognition accuracy of approximately 80% for both methods. A minor skewing of the images did not affect the recognition rate in any significant way.

A noted problem was that certain wood features, which the SURF method finds particularly interesting, are found at many different scale levels. This means that a tight cluster of features in one image can be falsely matched together with several scattered features in the other image,

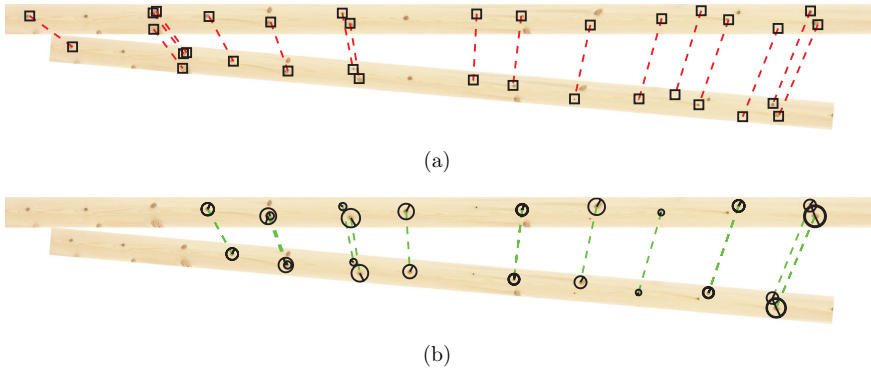


Figure 4.1: Example of a simulated distorted floorboard image which has been correctly identified in the database. (a) Block matching method. (b) SURF method.

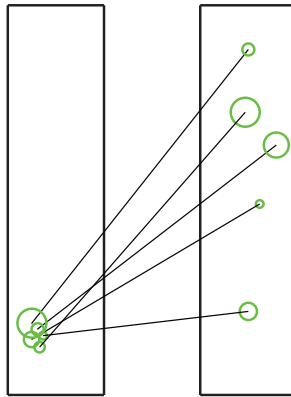


Figure 4.2: A tight cluster of features falsely matched to sparsely scattered features.

see Figure 4.2. This effect is most evident when the scaling of the images is anisotropic.

The two methods were found to be difficult to compare in a fair way, as they are quite different. The biggest difference probably being that the SURF method extracts features from several scale-levels. But the scale- and rotational independence of the SURF features did not prove to be advantageous in case of minor geometrical distortions.

The parameter settings of the two methods were chosen as they were, based on trying to get the methods to place at least one feature descrip-

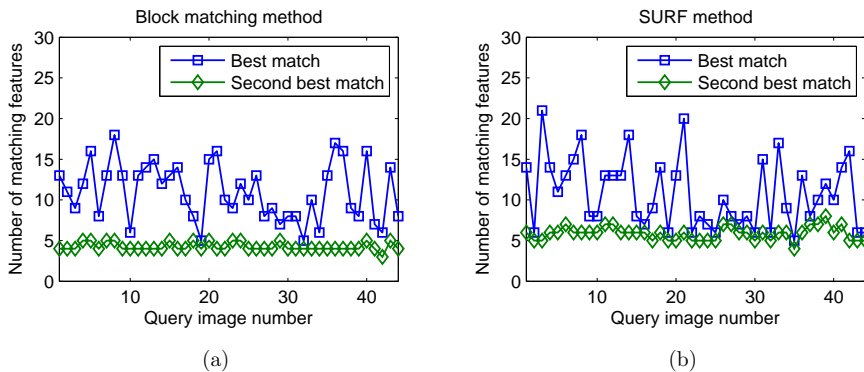


Figure 4.3: The number of matching feature points for the best matching floorboards compared to the second best match for each of the re-scanned floorboards. (Lines connect the measurement values for better visibility.) (a) Block matching method. (b) SURF method.

tor over each knot in the original and re-scanned images. There was no possibility to use the exact same corner detector, due to the closed implementation of SURF in MATLAB R2011b, or to get the same match acceptance thresholds to return the same amount of matches.

The number of descriptor matches was investigated for both methods on the re-scanned dataset. In Figure 4.3(a)-(b), the number of descriptor matches are plotted for the best and the second best match for the Block method and the SURF method, respectively. Where there is a small or negative difference between the best and second best match, there is a high likelihood of a failed matching. The Block method often has a slightly bigger difference compared to the SURF method, which shows up in the matching accuracy later. Notable is also that the two methods do not always perform similar on the same boards, which implies that they might complement each other.

## 4.2 Improvements

The FAST corner detector worked well on images without a black or white border around the edges of the boards. However, often with slightly rotated images or with slightly rough edges, a lot of unwanted “corners” were returned in these places. See a schematic example in Figure 4.4.

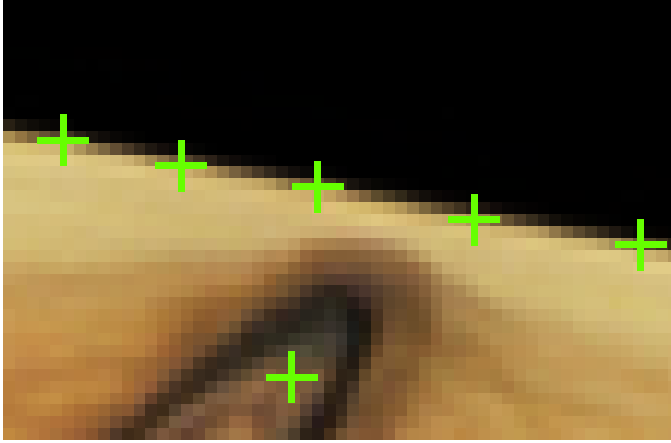


Figure 4.4: The FAST corner detector was found to often react to false corners along edges.

Table 4.1: Matching accuracy in % using entire board images as queries.

Dataset	Block I	SURF I	Block II	SURF II	Fused
Re-scanned	95.5	86.4	93.1	97.7	100.0
Canon	9.1	34.1	93.0	81.4	97.7

Thus, in Paper II, a switch to Harris corner detector was made.

In Table 4.1 a summary is shown of the results when matching whole boards for Paper I-II. The switch to Harris corner detector for the Block matching method dramatically increased the performance on the low resolution Canon dataset. However, the performance decreased slightly for the high resolution dataset, likely because fewer corners were extracted.

A lowering of the blob detection threshold also increased the performance significantly for the SURF method on the Canon dataset.

Especially the combined, Fused method, performs well on both datasets.

Both the Block and SURF methods extract more than double the amount of feature points on the high resolution dataset compared to the low resolution dataset. The more blurry images do not have the same distinct and sharp corners as the high resolution dataset and therefore fewer interest points are found. However, a blurred image can sometimes smooth out noise which otherwise could have lowered the results.

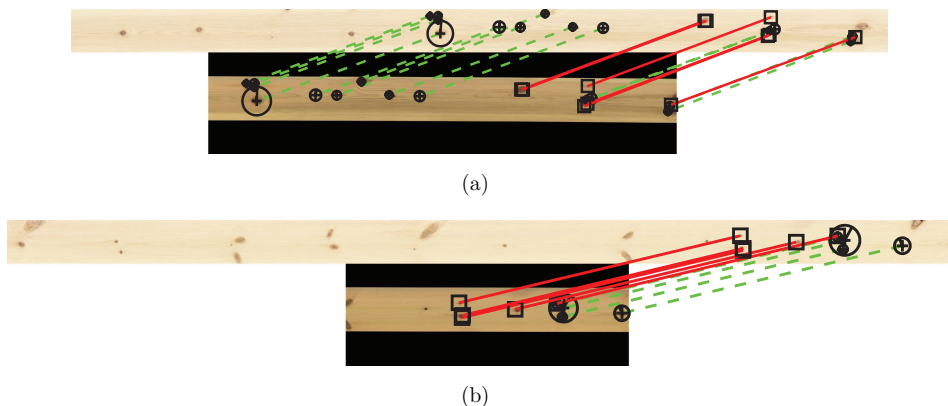


Figure 4.5: Two examples where the fused method correctly matched a cropped query image to the database image. The solid red lines connect Block features and the dashed green lines connect SURF features. The length of the database images have also been cropped here to better fit within the page. (a) Example 1. (b) Example 2.

### 4.3 Matching smaller image pieces

In Figure 4.5, two examples are shown where the Fused method correctly matched the smaller images to its corresponding database image. On some boards the Block matching method works better and on other boards the SURF method works better.

The matching accuracy depends on how many interest points are found, and therefore also on how many knots there are on the boards. To show this relationship, the average matching accuracy is plotted against the number of knots for the three different methods in Figure 4.6(a)-(b), for the high quality and low quality dataset, respectively.

The fusion of the two methods performs best overall and reaches 100% matching accuracy for board pieces with more than 20 knots for both datasets. For the low quality dataset, the matching accuracy seemingly drops a little when boards contain more knots. This drop was caused by one of the boards, where the majority of the features were falsely matched. This problem could likely be dealt with by allowing feature descriptors to have more than one match each.

Noteworthy is that the simple Block matching method has a substantially higher performance on the lower resolution, blurry, digital photos

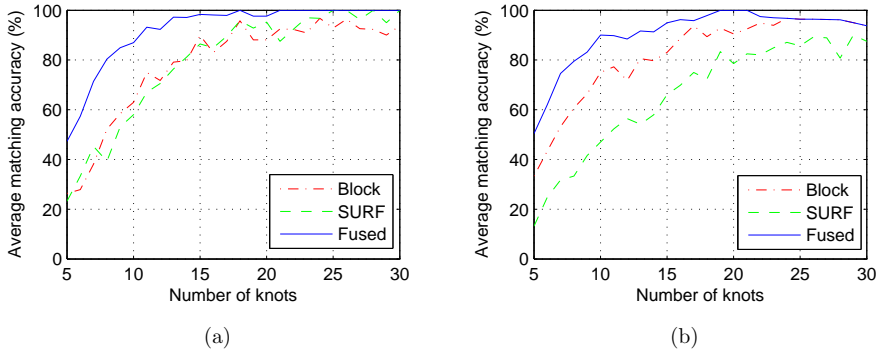


Figure 4.6: (a) Matching accuracy of subsets of the Re-scanned floorboards. (b) Matching accuracy of subsets of the digital photos.

compared to the SURF matching method. Probably, the interest point detector of SURF would need to be adjusted to extract more blobs on this dataset.

## 4.4 Matching panels using $K$ -plets

The results of the matching accuracy tests in Paper III are shown in Figure 4.7. From this figure, it can be seen that  $K = 6$  knot neighbors is the optimal value in this study. To obtain an accuracy of at least 99% with  $K = 6$ , the positional error standard deviation must not exceed 5 mm whilst detecting at least 85% of the knots. Detailed results with  $K = 6$  are shown in Table 4.2. The SSD threshold for accepting possible matches was set to  $\lambda = 1.4$ . That specific threshold was chosen since it resulted in the best overall performance of the algorithm. However, our tests showed that the performance of the algorithm was quite stable even when changing the parameter  $\lambda$  slightly.

When using  $K = 6$  and  $\lambda = 1.4$ , the tests of computational time showed that the average time of matching two panels to each other was 3.65 ms. Thus, if the database would contain 1000 panels, the average computational time for matching a query panel to such a database would be 3.65 s using our hardware setup (explained in Paper III), and our MATLAB implementation. This timing, at least gives a hint of what speeds could be reached.



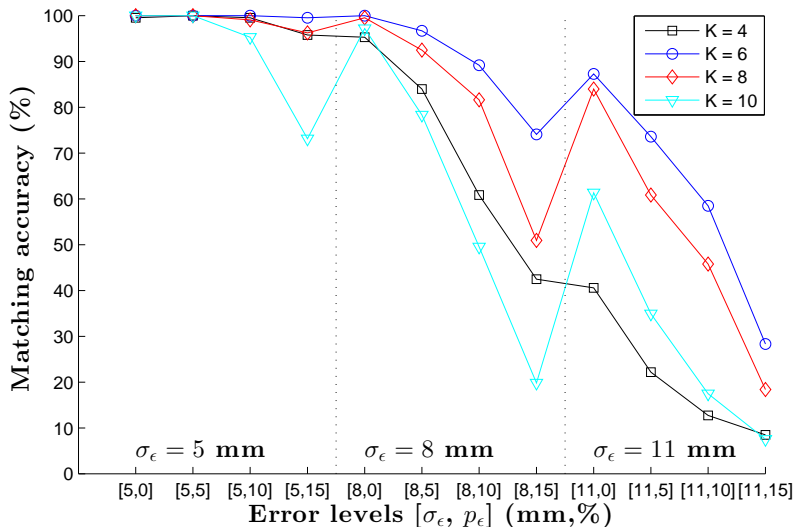


Figure 4.7: The matching accuracy for different number of knot neighbors,  $K$ , and different error levels. Error levels specified on the x-axis are: standard deviation of knot positional error,  $\sigma_\epsilon$ , and the percentage of knots removed,  $p_\epsilon$ . The measurement points are connected with lines for better visibility.

Table 4.2: Matching accuracy of the  $K$ -plet matching algorithm with  $K = 6$  knot neighbors and a SSD threshold for accepting matches  $\lambda = 1.4$ .

Accuracy (%)	100	100	100	99.5	100	96.7	89.2	74.1	87.3	73.6	58.5	28.3
Positional error (mm)	5	5	5	5	8	8	8	8	11	11	11	11
Removed knots (%)	0	5	10	15	0	5	10	15	0	5	10	15

The requirements on recognition rate, of course, varies from application to application. When matching panels in the Hol-i-Wood PR project, we need a recognition rate of more than 99% for the method to be usable. Our results show that such a level is possible to achieve using the proposed method if the error in knot position has a standard deviation of 5 mm or less. Furthermore, it is important that the knot segmentation is consistent on both the database image and the corresponding query image. Except for errors related to knot segmentation, the matching accuracy will also be affected by the size of the database and the frequency of knots.

According to the knot detection evaluation performed by Funck et al.

(2003), the performance of today's knot detection algorithms should be good enough for our panel recognition approach to be useful in some industrial applications.

---

---

# CHAPTER 5

---

---

## Conclusions

Paper I-II:

- Paper I-II proposes the use of feature detection methods to recognize sawn wood products having distinct features on their surfaces.
- When using feature detectors for recognition, there are many parameters which can be adjusted to receive different amounts, and different kinds, of feature points. The parameter settings will need to be calibrated and optimized for the specific material input.
- The fusion of the *Block matching method* and the *SURF method* improved the recognition rate of wooden boards substantially over the individual feature detection methods.
- Approximately 100% matching accuracy was obtained on our material for board pieces with more than 20 knots using both high- and low quality images.
- More than 90% matching accuracy was achieved for board pieces with more than 10 knots, using both high- and low quality images.
- The individual feature detection methods extract much more features from high quality images than from those of low quality.
- The recognition rate could be increased for boards with few knots by extracting more interest points, but at the expense of longer computation time.

Paper III:

- This paper presents a scale- and rotationally invariant algorithm for matching wooden panels based on internal knot structure. This novel approach opens up possibilities for a broad range of applications.
- For the Scots pine panels used in this study, the recognition algorithm was very successful, as should be the case for panels of other wood species that have a similar frequency of knots.
- The proposed algorithm uses knot positions; consequently the knot segmentation accuracy is very important. According to previous publications on knot segmentation (Funck et al., 2003), the proposed matching algorithm should be good enough for industrial applications.

---

---

# CHAPTER 6

---

---

## Future work

### **Feature detection**

Future work will include an industrial implementation of a panel recognition software that uses a combination of different feature detectors. A calibration framework is currently being developed to be able to optimize parameter settings to a specific input material. The aim of the optimization could either be high recognition accuracy, speed or a compromise between the two.

Many different feature detectors have been developed during the last decade, and a few new ones appear every year. There is a need to carry out a more extensive evaluation of their recognition performances on timber. However, the first step is to collect larger realistic image datasets of board/panel. Here, the Hol-i-Wood Patching Robot project will work as an important hub for data collection and testing. The advantage of feature detectors is that they work on every type of visible feature, be it a natural feature of wood, or a defect induced by rough handling.

### **Knot neighborhoods**

There are several variables which could be added to the knot neighborhood descriptors. These variables could include for example knot type, shape, size and relative orientation of knots. Adding more variables will probably have a great impact on the recognition of wood pieces with few knots.

### **Other approaches**

The best suitable recognition method will depend on the specific application. If there are differences in lengths of the products, maybe this is the best discriminating factor. With a multi-sensor approach using color, X-ray and tracheid effect, it would be easier to classify different features on sawn wood surfaces. Classified features and their positions would likely be very useful for recognition purposes.

---

---

# REFERENCES

---

---

- Anon, 1997: *Nordic Timber: Grading Rules for Pine and Spruce Sawn Timber, Pinus Silvestris, Picea Abies: Commercial Grading Based on Evaluation of the Four Sides of Sawn Timber*. Föreningen svenska sågverksmän (FSS), Sweden.
- Åstrand, E., 1996: *Automatic Inspection of Sawn Wood*. Linköping Studies in Science and Technology, Linköping University.
- Bay, H., A. Ess, T. Tuytelaars, and L. Van Gool, 2008: Speeded-Up Robust Features (SURF). *Computer Vision and Image Understanding*, **110** (3), 346–359.
- Belongie, S., J. Malik, and J. Puzicha, 2002: Shape matching and object recognition using shape contexts. *IEEE Trans. Pattern Anal. Mach. Intell.*, **24** (4), 509–522.
- Bijak, S., 2007: Tree growth-climate response in relation to habitat type in spruce stands of the borecka primeval forest. *TRACE-Tree rings in archeology, climatology and ecology*, **5**, 54–59.
- Birth, G. S., 1978: The light scattering properties of foods. *Journal of Food Science*, **43** (3), 916–925.
- Boukadida, H., F. Longuetaud, F. Colin, C. Freyburger, T. Constant, J. M. Leban, and F. Mothe, 2012: PithExtract: A robust algorithm for pith detection in computer tomography images of wood - Application to 125 logs from 17 tree species. *Computers and Electronics in Agriculture*, **85**, 90–98.
- Broman, N. O., J. Nyström, and J. Oja, 2008: Modelling the connection between industrially measured raw material properties and end user

- preferences. Part 2 - Results from preference studies. *Proceedings of the IUFRO Working Party 5.01.04, Joensuu, Finland*.
- Capon, B., 2005: *Botany for Gardeners*. EUi collection, Timber Press.
- Cerda, M., N. Hitschfeld-Kahler, and D. Mery, 2007: Robust tree-ring detection. *Advances in Image and Video Technology*, D. Mery and L. Rueda, Eds., Springer Berlin Heidelberg, Lecture Notes in Computer Science, Vol. 4872, 575–585.
- Dinwoodie, J., 1981: *Timber: Its Nature and Behaviour*. Van Nostrand Reinhold Company.
- Duncker, P. and H. Spiecker, 2009: Detection and classification of norway spruce compression wood in reflected light by means of hyperspectral image analysis. *IAWA Journal*, **30 (1)**, 59–70.
- Ek, M., G. Gellerstedt, and G. Henriksson, 2009: *Wood Chemistry and Wood Biotechnology (Pulp and Paper Chemistry and Technology)*, Vol. 1. de Gruyter.
- Estevez, P. A., C. A. Perez, and E. Goles, 2003: Genetic input selection to a neural classifier for defect classification of radiata pine boards. *Forest Products Journal*, **53 (7-8)**, 87–94.
- Funck, J., Y. Zhong, D. Butler, C. Brunner, and J. Forrer, 2003: Image segmentation algorithms applied to wood defect detection. *Computers and Electronics in Agriculture*, **41 (1-3)**, 157 – 179.
- Gjerdrum, P. and O. Hib, 2004: Heartwood detection in scots pine by means of heat-sensitive infrared images. *Holz als Roh- und Werkstoff*, **62 (2)**, 131–136.
- GoldenEye, 2014: Microtec GmbH, <http://www.microtec.eu>, last visited 2014-04-13.
- Hagman, O., 1996: On reflections of wood. wood quality features modelled by means of multivariate image projections to latent structures in multispectral images. Ph.D. thesis, Doctoral Thesis - Luleå University of Technology (Sweden).
- Hagman, O. and J. Nyström, 2003: Resin pocket detection on surfaces and in 3-d volumes of norway spruce. *Proceedings of the Fifth International*



- Conference on Image Processing and Scanning of Wood*, A. Rinnhofer, Ed., Joanneum research Forschungsgesellschaft mbH, 171–176.
- Harris, C. J. and M. Stephens, 1988: A combined corner and edge detector. *4th Alvey Vision Conference*, Manchester, 147–151.
- Hobbs, J. E., D. Bailey, D. L. Dickinson, and M. Haghiri, 2005: Traceability in the canadian red meat sector: Do consumers care? *Canadian Journal of Agricultural Economics/Revue canadienne d'agroeconomie*, **53** (1), 47–65.
- Jacobs, R. M., 1996: Product recall – a vendor/vendee nightmare. *Microelectronics Reliability*, **36** (1), 101 – 103.
- Johansson, E., D. Johansson, J. Skog, and M. Fredriksson, 2013: Automated knot detection for high speed computed tomography on pinus sylvestris l. and picea abies (l.) karst. using ellipse fitting in concentric surfaces. *Computers and Electronics in Agriculture*, **96** (0), 238 – 245.
- Kvarnström, B. and J. Oja, 2010: *Applications of RFID to Improve Traceability in Continuous Processes, Sustainable Radio Frequency Identification Solutions*, ISBN: 978-953-7619-74-9, InTech.
- Lamb, F. M., 1992: Splits and cracks in wood. *Proceedings of the 43rd Annual Meeting of Western Dry Kiln Association, Reno, NV. USA May 13-15*, 16–24.
- Lampinen, J., S. Smolander, O. Silven, and H. Kauppinen, 1994: Wood defect recognition: A comparative study. in: Workshop on machine vision for advanced production, Oulu, Finland, 2-3 June.
- Longuetaud, F., F. Mothe, B. Kerautret, A. Krhenbhl, L. Hory, J. Leban, and I. Debled-Rennesson, 2012: Automatic knot detection and measurements from x-ray {CT} images of wood: A review and validation of an improved algorithm on softwood samples. *Computers and Electronics in Agriculture*, **85** (0), 77 – 89.
- Lowe, D. G., 2004: Distinctive image features from scale-invariant keypoints. *International Journal of Computer Vision*, **60** (2), 91–110.
- Lycken, A., 2006: *Appearance Grading of Sawed Timber*. Doctoral thesis / Luleå University of Technology, Luleå tekniska universitet/LTU Skellefteå/Träteknologi.

- Moe, T., 1998: Perspectives on traceability in food manufacture. *TRENDS IN FOOD SCIENCE & TECHNOLOGY*, **9**, 211–214.
- Norell, K., 2011: Automatic counting of annual rings on pinus sylvestris end faces in sawmill industry. *Computers and Electronics in Agriculture*, **75** (2), 231 – 237.
- Norell, K. and G. Borgefors, 2008: Estimation of pith position in untreated log ends in sawmill environments. *Computers and Electronics in Agriculture*, **63** (2), 155–167.
- Nyström, J. and O. Hagman, 1999a: Methods for detecting compression wood in green and dry conditions. *Polarization and Color Techniques in Industrial Inspection*, E. Marszalec and E. Trucco, Eds., SPIE - International Society for Optical Engineering, 287–294, Proceedings of SPIE, the International Society for Optical Engineering.
- Nyström, J. and O. Hagman, 1999b: Real-time spectral classification of compression wood in *Pinus abies*. *Journal of Wood Science*, **45** (1), 30–37.
- Nyström, J., J. Oja, and N. O. Broman, 2008: Modelling the connection between industrially measured raw material properties and end user preferences. Part 1 - The simulation tool. *Proceedings of the IUFRO Working Party 5.01.04, Joensuu, Finland*.
- Oja, J., N. O. Broman, and J. Nyström, 2008: Modelling the connection between industrially measured raw material properties and end user preferences. Part 3 - Optimizing the industrial production. *Proceedings of the IUFRO Working Party 5.01.04, Joensuu, Finland*.
- Pahlberg, T. and O. Hagman, 2012: Feature recognition and fingerprint sensing for guiding a wood patching robot. *World Conference on Timber Engineering*, P. Quenneville, Ed., 724–733.
- Panshin, A. and C. De Zeeuw, 1970: *Textbook of Wood Technology: Structure, identification, uses, and properties of the commercial woods of the United States and Canada*. The American forestry series, McGraw-Hill.
- Patricio, M., D. Maravall, L. Usero, and J. Rejn, 2005: Crack detection in wooden pallets using the wavelet transform of the histogram of connected elements. *Computational Intelligence and Bioinspired Systems*, J. Cabestany, A. Prieto, and F. Sandoval, Eds., Springer Berlin Heidelberg, Lecture Notes in Computer Science, Vol. 3512, 1206–1213.

- Regattieri, A., M. Gamberi, and R. Manzini, 2007: Traceability of food products: General framework and experimental evidence. *Journal of Food Engineering*, **81** (2), 347 – 356.
- Rosten, E. and T. Drummond, 2006: Machine learning for high-speed corner detection. *European Conference on Computer Vision*, Vol. 1, 430–443.
- Russell, S. J. and P. Norvig, 2003: *Artificial Intelligence: A Modern Approach (2nd Edition)*. Prentice Hall.
- Schmid, C., R. Mohr, and C. Bauckhage, 2000: Evaluation of interest point detectors. *International Journal of Computer Vision*, **37** (2), 151–172.
- Skog, J. and J. Oja, 2010: Heartwood diameter measurements in pinus sylvestris sawlogs combining x-ray and three-dimensional scanning. *Scandinavian Journal of Forest Research*, **24** (2), 182–188.
- Sohal, A. S., 1997: Computerised parts traceability: An implementation case study. *Technovation*, **17** (10), 583 – 598.
- Taverniers, I., M. D. Loose, and E. V. Bockstaele, 2004: Trends in quality in the analytical laboratory. ii. analytical method validation and quality assurance. *TrAC Trends in Analytical Chemistry*, **23** (8), 535 – 552.
- Todoroki, C., E. Lowell, and D. Dykstra, 2010: Automated knot detection with visual post-processing of douglas-fir veneer images. *Computers and Electronics in Agriculture*, **70** (1), 163 – 171.
- Uusijärvi, R., 2000: Automatic tracking of wood. Ph.D. thesis, Kungliga Tekniska Högskolan, institutionen för produktionssystem.
- Walker, J., 2006: *Primary Wood Processing: Principles and Practice*. SpringerLink: Springer e-Books, Springer.
- Wangaard, F., 1981: *Wood: Its Structure and Properties*. Clark C. Heritage Memorial series on wood, Pennsylvania State University.
- Wood Resources International, 2013, 2013: Wood Resources Quarterly, Global Sawlog Prices.
- WoodEye, 2014: Innovativ Vision AB, <http://www.woodeye.se>, last visited 2014-04-13.



# Part II



---

---

# PAPER I

---

---

## Feature Recognition and Fingerprint Sensing for Guiding a Wood Patching Robot

**Authors:**

Tobias Pahlberg and Olle Hagman

**Reformatted version of paper originally published in:**

World Conference on Timber Engineering, 2012

© 2012, Proceedings of WCTE 2012. Reprinted with permission.





# FEATURE RECOGNITION AND FINGERPRINT SENSING FOR GUIDING A WOOD PATCHING ROBOT

Tobias Pahlberg<sup>1</sup>, Olle Hagman<sup>2</sup>

**ABSTRACT:** This paper includes a summary of a few commonly used object recognition techniques, as well as a sensitivity analysis of two feature point recognition methods. The robustness was analyzed by automatically trying to recognize 886 images of pine floorboards after applying different levels of distortions. Recognition was also tested on a subset of 5% of the boards which were both re-scanned using a line scan camera and photographed using a digital camera. Experiments showed that both the *Block matching method* and the *SURF method* are valid options for recognizing wood products covered with distinct features. The Block matching method outperformed the SURF method for small geometric distortions and moderate radiometric distortions. The SURF method, in its turn, performed better compared to the other method when faced with low resolution digital images.

**KEYWORDS:** Wood, Feature recognition, Fingerprint, Hol-i-Wood PR, Patching robot, Image analysis, Classification, Holonic, Sensor fusion

## 1 INTRODUCTION

Suppose a wooden board has gotten a crack, a few dead knots have loosened, and maybe the hue of a part of the board has changed. The question is if it is possible for a machine vision system to identify the board using only its biometric “fingerprint”? We may want to trace back through the history of the board. How was it produced and under what conditions? Or perhaps the task is merely to detect if the right piece has arrived at the right machine?

The objective of the presented work is to determine if it might be possible find a certain wooden board in a database of a thousand boards; and to determine a feasible type of descriptor that a computer can use to recognize boards. The descriptors need to be robust to both radiometric and geometrical distortions to be able to recognize a particular wood piece using different cameras and different camera setups.

The *Hol-i-Wood Patching Robot* project started in early 2012 and is a collaboration between Luleå University of Technology (LTU), TU Wien and TU München, as well as industrial partners; MICROTEC, Springer, TTTech and LIP BLED. The project will have resulted after three

years in several different standalone holonic modules of which the wood fingerprint recognition is one part.

The hardware will consist of a new multi-sensor scanner, a system for transport of laminated wood products which need repairing, and lastly a patching robot. The patching robot will be equipped with a vision system and should be able to recognize previously scanned wood pieces at the repair station, preferably using a non-invasive method. The patching robot will drill out certain defects and replace them with fitted wooden dowels. Defects such as dead knots, pitch pockets and geometrical defects. The identification using the fingerprint of wood is needed to inform the patching robot of which piece has arrived.

A number of laminated wooden end-products nowadays depend on a skilled machinist to repair the defects off-line, which can become a bottleneck in the production chain.

## 2 THEORY

The purpose of this chapter is to summarize and describe a few important concepts related to identification systems.

### 2.1 FINGERPRINTS

Within the field of biometrics the human fingerprint has been used for identifying people for over a century [1]. Scanning technology and algorithms have been pushed forward mainly by security and forensics applications. The procedures in fingerprint recognition software most

<sup>1</sup> Tobias Pahlberg, PhD Student, Wood Products Engineering, Luleå University of Technology, Forskargatan 1, 931 87 Skellefteå, Sweden. Email: tobias.pahlberg@ltu.se

<sup>2</sup> Olle Hagman, Professor, Wood Products Engineering, Luleå University of Technology, Forskargatan 1, 931 87 Skellefteå, Sweden. Email: olle.hagman@ltu.se

often have to address the following four design challenges [2]:

1. Image acquisition
2. Fingerprint representation
3. Feature extraction
4. Matching

Human fingerprint systems often rely on extracting certain minutiae or details for identifying individuals [1]. Ridge endings, ridge bifurcations and singular points are usual descriptors together with the coordinates and the orientation of these descriptors. Similar techniques can likewise be applied to identify wooden boards, where for example their knots and growth ring patterns describe "individuals" in the same way as the ridges do on a finger.

## 2.2 ROBUSTNESS

It can be very difficult to acquire an image under exactly the same conditions at different scanning stations. Furthermore, a lot of things can have happened to an object over time since a previous scan. Hence, a practical identification system needs to be robust to noise and distortions.

Geometric distortions can arise if for example a wooden board is transported skew past a line scan camera, if the pixels are non-square, or if the cameras have different poses at different scanning stations. Moreover, radiometric distortions introduced by different lighting conditions could be present, and at some manufacturers, for example, sawdust or dirt can occlude parts of the boards.

## 2.3 SPEED

A common way to reduce the problem of quickly having to search through a huge database of fingerprints to find a match is to group similar prints into bins [1]. These bins can be used for classification purposes if desired, but they can also be used to reduce the search space in a matching stage.

Bin sorting methods can on the other hand lead to problems if noise is present, where some features can become ambiguous. In such a case the sought board might have been put into the wrong bin and is therefore impossible to find.

Instead of sorting boards into discrete classes, a feature vector can be used to represent it. The Euclidean distance can then be calculated between the query vector and vectors in the database.

## 2.4 CLASSIFIERS

Neural networks (NN) are widely used as a classification method for fingerprints. A fingerprint system called PCASYS which utilizes NNs was developed for the FBI in the early 1990s [3].

Feature extraction and classification of wood defects was done using NNs in [4, 5]. The learning problem in those cases was solved by the use of self-organizing maps (SOM) in the early feature extraction stages. A correct

classification rate of 86%, for example, was obtained using Gabor filters and adaptive color histograms.

A tree-structure support vector machine (SVM) approach was proposed in [6] to classify four types of wood knots, achieving an average correct classification rate of 96.5%. In a related thesis work a supervised classifier was trained with Adaboost to classify different stain type defects on wood in [7].

Different classifiers have different strengths and weaknesses; hence a combination of classifiers is often the best solution.

## 2.5 OBJECT RECOGNITION

Object detection, classification and recognition are tightly intertwined areas. The sought output is different for them, but the process of getting the output is usually similar. Often the procedure involves extraction of *feature points* from the objects.

A feature point is a region in an image that is likely to be recognized in other images [8]. Typical feature points include, for example, corners, blobs and T-junctions. Corners, i.e., positions in an image where there is a strong intensity change in two orthogonal directions, are very good objects to track [9, 10].

A region around the corner is usually stored. These regions, or templates, are later used for recognition of objects by finding several matching regions between images.

Criteria for good feature points, or *interest points*, are described in [11]:

1. *Distinctness*: The points should be distinguishable from their neighborhood, e.g., consist of a pronounced gradient in intensity or color.
2. *Invariance*: The points should be invariant with respect to expected geometric and radiometric distortions.
3. *Stability*: The points should be robust to noise.
4. *Seldomness*: There should not be several similar points in the same image to avoid confusion. (If a point is part of a repetitive pattern, the possibility for a false match is high.)
5. *Interpretability*: The points should preferably be interpretable, such as an edge, corner or blob.

Edges are usually not good interest points; the region information is similar along the line and hence does not fulfil the seldomness requirement. Smooth untextured regions do not uphold the distinctness requirement, et cetera.

Several corner- and feature point-detection algorithms have been produced over the years. One of the most famous corner detectors is the Harris corner detector [12]. The Harris method involves moving a search window over a grayscale image and computing the weighted Sum of Squared Difference (SSD) between the starting location and its surroundings (Figure 1).

In a smooth untextured part of the image there will not be a big SSD response in any direction. At a line, or a sharp gradient change, there will be a big response in

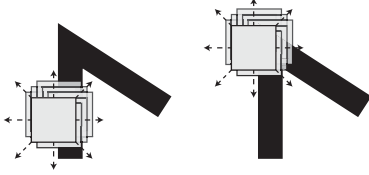


**Figure 1:** Harris corner detector computing a weighted SSD between the starting location and its surroundings. A line is found to the left, a corner to the right.

one direction. At a corner there will be a big response in two different directions.

If a grayscale image is denoted  $I$ , the search window area  $(u, v)$ , and the shift  $(x, y)$ , then the weighted SSD is given by:

$$D(x, y) = \sum_{u, v} w(u, v) (I(u+x, v+y) - I(u, v))^2. \quad (1)$$

The weighting factors,  $w(u, v)$ , are often formed to create a circular search window. Moreover, a Gaussian smoothing can be applied over the region to counter the noise introduced due to the discrete grid of pixels in an image.

By use of Taylor expansion, Equation (1) can approximately be rewritten as:

$$D(x, y) \approx (x \ y) A \begin{pmatrix} x \\ y \end{pmatrix}, \quad (2)$$

where

$$A = \sum_{u, v} w(u, v) \begin{bmatrix} \frac{\partial^2 I(u, v)}{\partial x^2} & \frac{\partial^2 I(u, v)}{\partial x \partial y} \\ \frac{\partial^2 I(u, v)}{\partial y \partial x} & \frac{\partial^2 I(u, v)}{\partial y^2} \end{bmatrix}. \quad (3)$$

Second derivatives are better suited for finding lines and corners than first derivatives, i.e., gradients. Second derivatives are only non-zero at places in the image where there is a gradient change, not where there is a constant gradient. A constant gradient is usually not defined as a line.

Most corner detectors utilize the Hessian matrix, in some way, to find intensity maxima.

Through the eigenvalues,  $\lambda_1$  and  $\lambda_2$ , of  $A_{2 \times 2}$ , a rotationally invariant descriptor of what is going on around a point in an image is obtained.

1. If both  $\lambda_1$  and  $\lambda_2$  are large, a corner is present in the region.
2. If one eigenvalue is large and the other is small, then a line is present in the direction perpendicular to the eigenvector with large eigenvalue.
3. If both  $\lambda_1$  and  $\lambda_2$  are small, there is no a distinct edge or corner in that region.

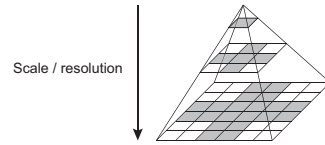


**Figure 2:** The image pyramid of scale.

The eigenvalues are usually not computed explicitly due to the computational cost. Instead the trace and determinant of  $A$  can be used.

In the method proposed by Shi and Tomasi, a threshold is set on the smaller of the two eigenvalues which decides if a corner is accepted [13].

Another corner detector, the Features from Accelerated Segment Test (FAST, [14]), uses a different approach. The algorithm searches for patches within an image that “looks” like a corner. Hence, it does not have to calculate second derivatives or eigenvalues. As can be understood by its abbreviation, it is fast, and trades exactness for speed. Only four pixels are traversed in each patch when deciding the probability of there being a corner in it. Only in the most probable patches, a more thorough investigation is made by traversing more pixels around the circumference of the patch. The FAST corner detector is often accurate enough, as long as there is not too much noise in the image.

Lowe proposed a novel approach for feature point detection called Scale-Invariant Feature Transform (SIFT, [15]). SIFT detects the dominant gradient orientation of interest points in an image and saves the gradient information around these points. Since the dominant orientation is found, the method becomes rotationally invariant. SIFT features can also be matched at different scales since the images are downsampled iteratively while leaving the kernel size unchanged. Scales are divided into so-called *octaves*, where the next octave corresponds to a doubling of the length of the side of the image (Figure 2). Moreover, SIFT and its variants can handle some variation in illumination of the scene.

A fast and robust method which is in many ways similar to SIFT is the Speeded-Up Robust Features method (SURF, [16]). SURF uses integral images [17] for fast calculations of sums of intensities over rectangular regions in grayscale images. The use of integral images makes it possible to do such computations in constant time, independent of region size. In the SURF approach, the kernel sizes are resized instead of the images, as in SIFT. A Hessian matrix-based method is used for finding corners and blobs suitable as feature points.

Intensity information on feature points is stored in a way similar to SIFT. However, SURF is by default using half as much storage space, i.e., a 64-dimensional vector instead of 128. This speeds up both the feature extraction and the matching time.

For images without distinct features, a template-based approach may be more suitable. *Template matching* works by moving a search window over an image while calculating an error metric, e.g., SSD or normalized cross correlation between the template and search image.

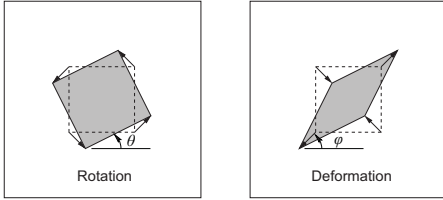


**Figure 3:** A planar affine transformation consists of a rotation (left), and a deformation (right). Illustration from [18].

The minimum error, or maximum response, is given when the template is at the correct location.

## 2.6 GEOMETRIC TRANSFORMATIONS

The geometric relation between points in space and a two-dimensional image can be described by a *projective* transformation [18]. If most of the points in a scene are at the same depth, and if a long focal length is used, then the *affine* transformation is a good approximation of the projective transformation. Affinely distorted images can be generated using the planar affine transformation. This 2D to 2D transformation skews the image and then rotates and translates it (Figure 3). The transformation preserves straight lines, i.e., lines which were parallel, will be parallel also after the transformation. Furthermore, affine transformations preserve the length ratios between parallel line segments in an image, as well as ratios between areas.

The planar affine transformation  $\mathbf{x}' = H_A \mathbf{x}$  is defined as:

$$\begin{pmatrix} x' \\ y' \\ 1 \end{pmatrix} = \begin{pmatrix} a_{11} & a_{12} & t_x \\ a_{21} & a_{22} & t_y \\ 0 & 0 & 1 \end{pmatrix} \begin{pmatrix} x \\ y \\ 1 \end{pmatrix} = \begin{pmatrix} A & \mathbf{t} \\ \mathbf{0}^T & 1 \end{pmatrix} \mathbf{x}. \quad (4)$$

The linear transformation,  $A$  in Equation 4, consists of a deformation followed by a rotation:

$$A = R(\theta)R(-\varphi)DR(\varphi). \quad (5)$$

After the first rotation,  $\varphi$ , the image is scaled in  $x$ - and  $y$ -directions using the diagonal matrix in Equation 6, skewing the image.

$$D = \begin{pmatrix} \lambda_1 & 0 \\ 0 & \lambda_2 \end{pmatrix} \quad (6)$$

The image is then rotated back by the same amount and a different rotation,  $\theta$ , is applied. Lastly, a translation by  $(t_x, t_y)$  is applied to the image.

## 3 MATERIALS AND METHODS

### 3.1 IMAGES AND IMAGE ACQUISITION

The chosen dataset consists of 886 floorboards from Scots pine (*Pinus sylvestris*) with the dimension 21x137 mm. The same set of floorboards was previously used in [19-21]. They are between 3007-5109 mm long, with a mean length of approximately 4500 mm. The boards were sawn from 222 logs with top diameter between

201-215 mm and were randomly collected from Bollsta sawmill in central Sweden. The boards had been planed, sanded and finished with white pigmented oil and a thin layer of varnish.

The finished floorboards were scanned in 2006 using a high resolution color line scan camera; Dalsa Trillium TR-37. It is a 3CCD camera with a 2048 pixel array for each of the colors; red, green and blue [19]. The boards were scanned at a resolution of 2.5 pixels/mm lengthwise and 10 pixels/mm across. Photocells were set up to automatically crop off 80 mm from each side to avoid edge artifacts. The images were then resized to a resolution of 1 pixel/mm in both directions using bi-cubic interpolation and were saved in JPEG format at 95% quality. The colors of the images had been carefully calibrated to match the colors of the boards in reality.

### 3.2 ROBUSTNESS TESTING

To test the robustness of the two different feature-matching techniques, a two-level full factorial experiment was created. A subset of 100 floorboards was picked out randomly from the total 886. The planar affine transformation was used to distort these images using different parameter combinations. The four parameters;  $\theta$ ,  $\varphi$ ,  $\lambda_1$  and  $\lambda_2$ , were each assigned a “low” and a “high” value. Hence,  $2^4 = 16$  new image datasets containing 100 images each were created to test all combinations and to determine which factors had the most significant impact on the identification accuracy. The different low and high values can be seen in Table 1.

**Table 1:** The affine distortion parameters’ “low” and “high” value used in the robustness testing.

	$\theta$ (°)	$\varphi$ (°)	$\lambda_1$	$\lambda_2$
Low	5	5	0.9	0.9
High	15	15	0.7	0.7

The translation parameters of the affine transformation were set to zero since they would not affect the result in any case. Feature points are matched independently of their positions and only their relative positions in each image are used to sort out false matches.

The low and high values were chosen accordingly after screening experiments indicated difficulties within these ranges.

Note that when the scaling parameters,  $\lambda_1 = \lambda_2 = 1$ , there is no scaling done. As can be seen in Table 1, a 10% size reduction is chosen as the low value, and a 30% size reduction as the high value.

Anti-aliasing is used to limit the impact of aliasing on the output images when resizing and transforming images. Aliasing may appear as “stair-step” patterns at lines in an image or as moiré patterns, a ripple- or wave-type artifact.

### 3.3 RE-SCAN OF IMAGES

The same line scan camera as before was used in 2012 to re-scan 5% of the floorboards to have a subset of realistically acquired images to test the matching capabilities on. Some of the boards had during the past

years of storage become somewhat crooked or bowed. Moreover, no stabilization of the boards was carried out while the conveyor belt was transporting them past the camera at the re-scan. No color corrections were made on the images and some dust stains were present on a few of the floorboards.

This time the camera was mounted at such a distance from the conveyor belt that yielded a resolution of 5.6 pixels/mm lengthwise and 6.5 pixels/mm across. The entire lengths of the board images were kept this time, and the images were resized to 1 pixel/mm in both directions using bicubic interpolation. They were saved in JPEG format at maximum quality.

### 3.4 DIGITAL PHOTOS

To provide a last tough challenge to the recognition methods, digital photos were taken of the floorboards from a distance. The photos were acquired with a Canon 400D camera at a resolution 0.6 pixels/mm. The images were scaled up to 1 pixel/mm in order not to disadvantage the scale-dependent Block matching method.

### 3.5 FEATURE EXTRACTION AND MATCHING

Two different methods were used for feature extraction and matching in the experiments. The first is referred to as the *Block matching method* and the other as the *SURF method*. Implementations of these methods can be found

as open source [22], and are often used for similar purposes in other computer vision applications.

In this paper, implementations from MATLAB® R2011b, Computer Vision System Toolbox™, have been incorporated.

#### 3.5.1 Block matching method

In the Block matching method simple square neighborhoods are extracted as features around interesting points in an image. A detailed explanation is presented in Algorithm 1.

A few settings for the FAST corner detector were altered from the default. The size of the search window for finding corners was set to 25x25 pixels, i.e., 25x25 mm due to the resolution. The corner threshold parameter was increased to 0.001 (default: 0.0005) to pass along also weaker corners. However, the intensity threshold for accepting corners was instead increased to 20 (default: 0.1) out of the maximum 127.5, to reduce the number of corners being falsely detected on the boards' boundaries. No more than the 50 best corners were kept to be able to execute the matching step within reasonable time.

The intensity information in a 25x25 pixel neighborhood around each FAST point was extracted as feature points. This neighborhood size was chosen since it encircled most of the knots.

The MATLAB-function *matchFeatures* carries out steps

---

#### Algorithm 1: Block matching method

---

1. Run FAST corner detector on query image,  $I_A$ , and database image,  $I_B$ .
  2. *Description of feature points:*
    - 2.1. Extract the intensity information in a square patch around the corners.
    - 2.2. Patches that are on the border or completely outside the region of interest are removed.
    - 2.3. Reshape the patches into  $n_A$  and  $n_B$  column vectors and insert them as the columns of feature matrices  $A$  and  $B$ .
    - 2.4. Normalize the columns of  $A$  and  $B$  to make the method more robust to radiometric differences.
  3. *Matching:*
    - 3.1. Calculate the  $(n_A \times n_B)$  error matrix between all the features in  $A$  and  $B$  using SSD according to:
 
$$E(i, j) = \sum \left( (\mathbf{a}_i - \mathbf{b}_j) \cdot \mathbf{a}_i \right)^2$$
, where  $\mathbf{a}_i$  and  $\mathbf{b}_j$  are the column vectors of  $A$  and  $B$  respectively, and the operator  $(\cdot)^2$  squares every element in a vector.
    - 3.2. For every row in  $E$ , find the lowest column error, i.e., the best matching features between  $I_A$  and  $I_B$ .
    - 3.3. Remove duplicate feature pairs.
    - 3.4. Remove weak matches which have an error above some specified threshold.
- 

---

#### Algorithm 2: SURF method

---

1. Create a scale-space representation of the query image and the database image by use of integral images and box filters.
  2. *Detection of feature points:*
    - 2.1. Use the local maxima of the Hessian determinant operator applied to the scale-space to obtain feature points.
    - 2.2. Keep points with a response level above a certain threshold.
    - 2.3. Refine scale and location of these candidates.
    - 2.4. SURF points which are on the border or completely outside the region of interest are removed.
  3. *Description of feature points:*
    - 3.1. Calculate a dominant orientation direction using the neighborhood gradient information to make the feature points rotationally invariant.
    - 3.2. Build a 64-dimensional descriptor corresponding to the local normalized gradient histograms using Haar wavelets.
  4. *Matching:*
    - 4.1. Compute the Euclidean distance between all potential matching pairs.
    - 4.2. Reduce mismatches using a nearest neighbor distance ratio criterion.
-

3.1-3.4 in the Block matching algorithm. There, the SSD boundary for accepting matches was increased to 2% instead of the default, 1%, to produce more potential matches. Feature pairs with a matching error above this percentage are removed.

### 3.5.2 SURF method

The SURF method is thoroughly described in [16], and an extensive algorithm description can be found in [23]. A shortened version is presented in Algorithm 2.

The number of octaves was kept at the default, 3, but the number of scale levels within each octave was increased to 6 (default: 4). No maximum number of SURF points was specified here, only the default metric threshold for accepting points was used.

The SSD boundary for accepting matches was increased to 5% instead of the default, 1%.

The MATLAB-function *matchFeatures* carries out steps 4.1-4.2 in the SURF algorithm.

### 3.6 REMOVAL OF FALSE MATCHES

Some features of wood, such as knots, can look quite similar, especially to a computer. Hence, features from one floorboard are sometimes matched to several features in another. This ambiguity can be taken care of by removing features that get a lot of matches (Sparsity requirement, Section 2.5). Features with more than three possible candidate matches were removed.

A problem can also be that the best fit of features, algebraically, might not be the correct one, for different reasons. Hence, it is usually a bad idea to sort out "erroneous" matches solely on the basis of a SSD threshold.

#### 3.6.1 Geometric Transform Estimator

MATLAB's Geometric Transform Estimator was utilized to remove point pairs that should be considered as false matches given a certain geometric transformation. The non-reflective similarity transformation was chosen instead of the affine transformation since it, due to fewer degrees of freedom, performed more stably.

To allow for some deviation and to loosen the demands

on the point pairs to conform to the model, the Euclidean pixel distance threshold was raised to 100 mm. Random Sample Consensus, RANSAC [24], was chosen as the method for determining inliers, i.e., true matches.

A description of the geometric transform estimator is presented in Algorithm 3.

## 4 RESULTS AND DISCUSSION

In this section the two different feature recognition methods are compared. Note, however, that their performances depend on parameters which do not always apply to both methods.

Test runs were carried out on a PC running Windows 7 64-bit with an Intel® Xeon® processor at 2.53 GHz.

It takes about 12 seconds to acquire feature points for one query floorboard and then compare it against the database of 886 floorboards, i.e., around 14 ms to compare it against one database-file. The Block matching method and the SURF method take roughly the same amount of time.

### 4.1 ROBUSTNESS TESTING

For every distorted image, the best matching board in the database was chosen based on having the greatest number of unique matching feature points.

Both the Block matching method and the SURF method successfully identified the correct individual in Figure 4. The identification accuracy of the two methods for different parameter combinations can be seen in Table 2. The Block matching method performs well as long as the scaling parameters are kept at the low level. The scaling in  $x$ -direction,  $\lambda_I$ , has the biggest impact on the accuracy. Inspection of some of the failed cases showed that occasionally the FAST corner detector misinterpreted sections of the boards' outer borders as corners and thus a lot of feature points were rejected. The worst case occurred at a large skewing angle,  $\phi$ , in conjunction with a large scaling in  $x$ -direction,  $\lambda_I$ . However, neither a large rotation angle nor a large skewing angle seems to correlate significantly with bad accuracy.

The SURF method's identification accuracy remains decent when the scaling parameters are kept at the lower level. However, the SURF method has big trouble when either  $\lambda_I$  or  $\lambda_2$  is at the high level. A noted problem is that certain wood features that the SURF method sees as especially interesting are found at many different scale levels. Thus, several scattered features in one image can be falsely matched together with a tight cluster of features in the other image. This effect is most evident when either of  $\lambda_I$  or  $\lambda_2$  is at the high level and the other one is not. The SURF method, however, does not experience the same problems of finding invalid feature points on edges of the boards.

A large number of matched feature points usually means that the correct board has been identified. If the second best matching board has almost the same amount of matched feature points, then the chances are high that the "best" might not be the correct one. To visualize the difference between the number of matched feature points for the best match and the second best match, for small geometric distortions, a box plot was created (Figure 5).

---

#### Algorithm 3: Geometric transform estimator

---

1. Loop until *maximum number of iterations* has been reached, or until enough inliers have been found.
    - 1.1. Randomly pick a number of matched point pairs from images  $I_A$  and  $I_B$  (2 pairs for non-reflective similarity transformation).
    - 1.2. Calculate the transformation matrix,  $H_S$ , using the relationship  $\mathbf{x}' = H_S \mathbf{x}$ .
    - 1.3. Project the points from one image onto the other and sum the Euclidean distances between the point pairs.
    - 1.4. Update  $H_S$  if the summed distance is lower than the previous minimum.
  2. Return a list of inlier point pairs.
-

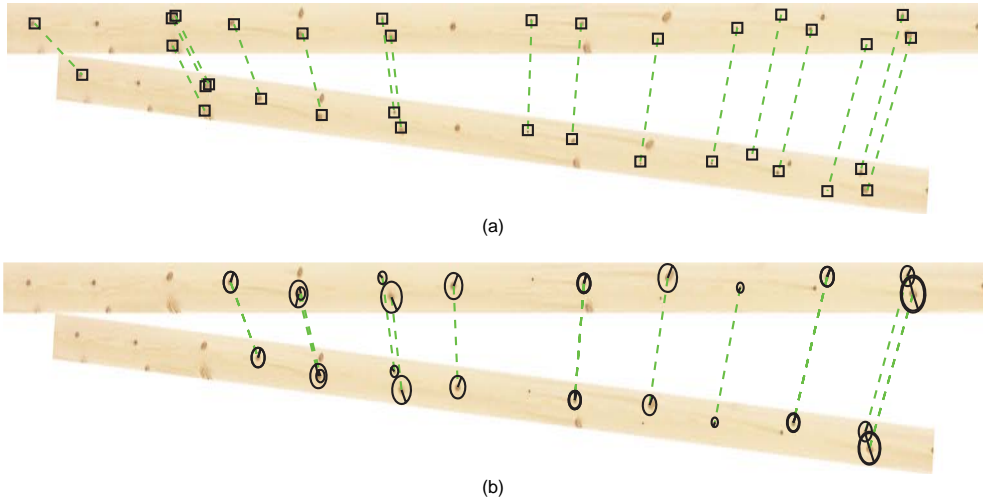


**Figure 4:** Example of a simulated distorted floorboard image with  $(\theta, \varphi, \lambda_1, \lambda_2) = (-5^\circ, -5^\circ, 0.9, 0.9)$  which has been correctly identified in the database. (a) Block matching method. (b) SURF method.

Each of the 886 floorboards was given a small geometric distortion and was then matched against the original images. The parameters of the affine transformation were assigned uniformly distributed random numbers on the intervals:  $-5^\circ \leq \theta$ ,  $\varphi \leq +5^\circ$  and  $0.9 \leq \lambda_1, \lambda_2 \leq 1.1$ . The plots show that the Block matching method has a slightly higher mean number of matched features for the best match.

#### 4.2 RE-SCANNED IMAGES

An example of how one of the re-scanned images could

look is shown in Figure 6. Both the Block matching method and the SURF method successfully identified the correct board also in that case.

The identification accuracy of the 44 re-scanned boards can be seen in Table 3.

The Block matching method outperforms the SURF method for this particular case comprising small geometric distortions and moderate radiometric changes. Due to the smaller geometric distortions in this experiment, the drawbacks of the two methods should not negatively affect the accuracy to the same extent.

**Table 2:** Comparison of the identification accuracy between the Block matching method and the SURF method for the simulated distorted images dataset at different maximum rotation angles and scaling parameters. The best accuracy is marked green for each method and the worst, red.

Block matching method		SURF method		$\theta$ ( $^\circ$ )	$\varphi$ ( $^\circ$ )	$\lambda_1$	$\lambda_2$
Accuracy (%)	Accuracy (%)	Accuracy (%)	Accuracy (%)				
93	98	5	5	0.9	0.9		
94	48	5	5	0.9	0.7		
90	36	5	5	0.7	0.9		
78	75	5	5	0.7	0.7		
94	98	5	15	0.9	0.9		
100	47	5	15	0.9	0.7		
68	35	5	15	0.7	0.9		
78	76	5	15	0.7	0.7		
97	92	15	5	0.9	0.9		
98	50	15	5	0.9	0.7		
78	36	15	5	0.7	0.9		
82	78	15	5	0.7	0.7		
100	93	15	15	0.9	0.9		
98	53	15	15	0.9	0.7		
96	28	15	15	0.7	0.9		
82	79	15	15	0.7	0.7		

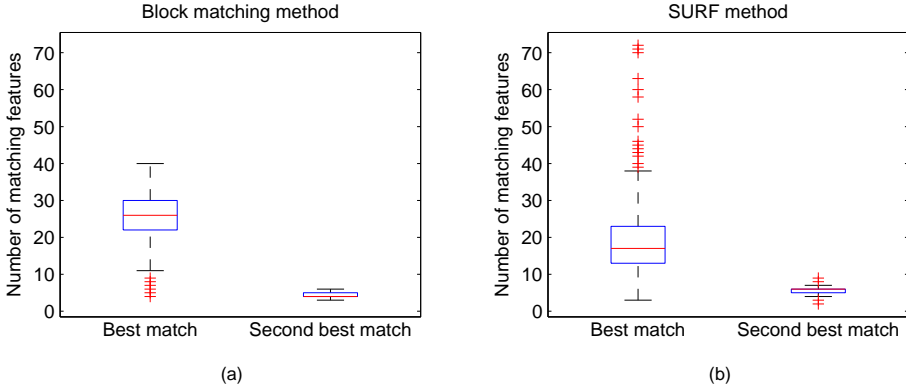


**Figure 5:** The number of matching feature points for the best matching floorboards compared to the second best match when:  $-5^\circ \leq \theta$ ,  $\varphi \leq +5^\circ$  and  $0.9 \leq \lambda_1$ ,  $\lambda_2 \leq 1.1$ . (a) Block matching method. (b) SURF method.

A visualization of the difference between the numbers of matched features for the best match and the second best match is shown for each of the 44 boards in Figure 7. The same tendency as before can be seen there. The SURF method has a more widespread number of matched features, though there is more often a smaller difference between the best and the second best match. This means that the SURF method can be seen as less robust in that sense.

**Table 3:** Comparison of the identification accuracy between the feature point methods for the re-scanned images.

Method	Accuracy (%)
Block matching	95.5
SURF	86.4

### 4.3 DIGITAL PHOTOS

The last and most challenging case was that of matching

low resolution digital images with the original, higher resolution, images. The digital images were cropped and scaled to match the resolution of the original images. The identification accuracy is shown in Table 4, where the SURF method is clearly the most robust method in this case.

Closer investigation showed that the FAST corner detector had trouble finding features in these images. Different settings were tested but did not produce more feature points. Hence the somewhat undesired poor result for the Block matching method.

**Table 4:** Comparison of the identification accuracy between the feature point methods for the digital photos.

Method	Accuracy (%)
Block matching	9.1
SURF	34.1

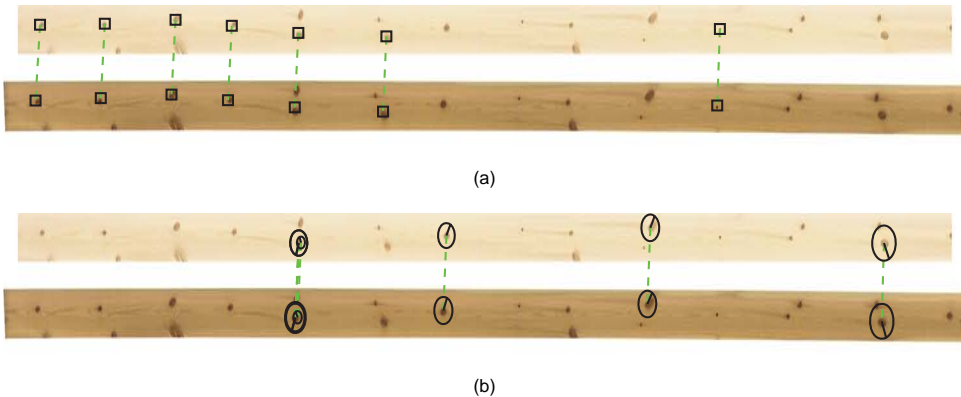


**Figure 6:** Example of a re-scanned floorboard image identified in the database. (a) Block matching method. (b) SURF method.



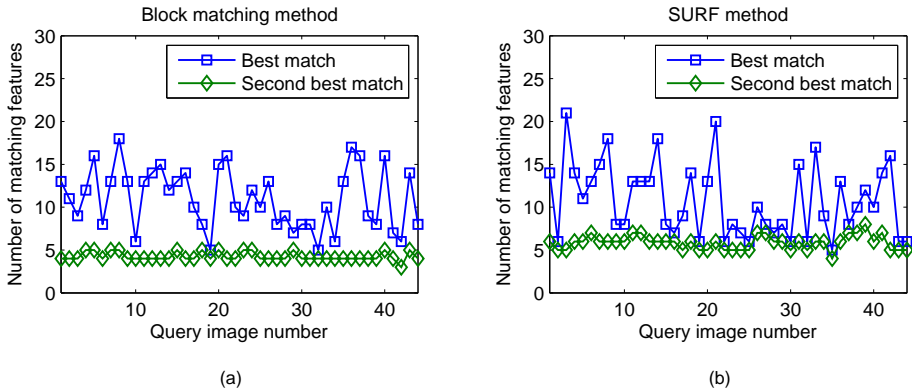


**Figure 7:** The number of matching feature points for the best matching floorboards compared to the second best match for each of the re-scanned floorboards. (a) Block matching method. (b) SURF method.

## 5 CONCLUSIONS

There are many parameters that can be varied and tweaked to get different amounts of feature points from the algorithms. If thresholds for accepting corners are lowered, more feature points will be returned. However, these will be less robust.

A drawback of having a lot of features is that the extraction and matching procedure will take longer, making a real-time application less feasible.

A problem with the FAST corner detector is that it can in some cases misinterpret jagged lines and edges as corners. The SURF method's corner detector is in this respect more reliable and better at finding features in an image.

The method of finding interest points using corners, i.e., a high second derivative response in two directions, is a very general method. It is widely used within machine vision in various different scenarios. A wooden surface with knots is a special case that probably should be dealt with using a more specialized knot-finding algorithm. The Block and SURF features are likewise common general purpose feature points, but not very specialized towards recognizing wood. The advantage of these methods is that they are quite robust. It would be easy to re-tune the parameters and apply the methods on a slightly different recognition problem.

The SURF method's problem of incorrectly matching several scattered features in one image to a tight cluster of features in the other image must be addressed. This is not a huge problem and can definitely be solved.

The Block matching method performed surprisingly well in all experiments, especially considering that it is scale and rotation dependent. The method would, however, greatly benefit from using a more robust knot-finding algorithm.

The rotationally invariant SURF method generally handled rotations worse than the Block matching method, which was unexpected. Rotational invariance is possibly not as crucial due to knot features being mostly rounded.

Both the Block matching method and the SURF method are valid options for recognizing wood products covered with distinct features. The Block matching method outperformed the SURF method for small geometric distortions and moderate radiometric distortions. The SURF method, in its turn, performed better compared to the other method when faced with low resolution digital images. However, the FAST corner detector often failed to acquire enough valid interest points to the Block matching method in this case.

A combination of Block- and SURF features would most certainly provide a big improvement in identification accuracy.

Future work will include the incorporation of multi-sensor data and defect classification used in existing systems for wood inspection.

## ACKNOWLEDGEMENTS

The authors would especially like to thank Olof Broman for giving us access to the floorboards used in this work. Also, thanks to Simon Dahlquist at SP Trä for assisting us with the re-scanning of the boards.

## REFERENCES

- [1] Yager, N. and Amin, A., Fingerprint classification: a review, *Pattern Analysis & Applications*, 7:77-93, 2004.
- [2] Jain, A., Hong, L., Pankanti, S., and Bolle, R., An identity-authentication system using fingerprints. *Proceedings of the IEEE*, 85:1365-1388, 1997.
- [3] Wilson, C., Massively parallel neural network fingerprint classification system, National Institute of Standards and Technology, 1992.
- [4] Lampinen, J., Smolander, S., and Korhonen, M., Wood surface inspection system based on generic visual features. In: International Conference on Artificial Neural Networks, ICANN'95, 1995.
- [5] Lampinen, J. and Smolander, S., Self-organizing feature extraction in recognition of wood surface defects and color images. *International Journal of*

- Pattern Recognition and Artificial Intelligence*, 10:97-113, 1996.
- [6] Gu, I., Andersson, H., and Vicen, R., Wood defect classification based on image analysis and support vector machines. *Wood Science and Technology*, 44:693-704, 2010.
- [7] Jabo, S., Machine vision for wood defect detection and classification, Masters thesis, Chalmers tekniska högskola, 2011, <http://publications.lib.chalmers.se/records/fulltext/136883.pdf>, last visited 2012-03-08.
- [8] Börlin, N. and Igasto, C., 3D measurements of buildings and environment for harbor simulators, Technical Report 19, Umeå University, Department of Computing Science, 2009.
- [9] Bradski, G. and Kaehler, A., *Learning OpenCV*, O'Reilly Media Inc., 2008.
- [10] Moravec, H., Obstacle avoidance and navigation in the real world by a seeing robot rover. In: Tech. report CMU-RI-TR-80-03, Robotics Institute, Carnegie Mellon University & doctoral dissertation, Stanford University, number CMU-RI-TR-80-03, 1980.
- [11] Förstner, W., A feature based correspondence algorithm for image matching. *International Society for Photogrammetry and Remote Sensing*, 26:150-166, 1986.
- [12] Harris, C. and Stephens, M., A Combined Corner and Edge Detection. In: Proceedings of the Fourth Alvey Vision Conference, 147-151, 1988.
- [13] Shi, J. and Tomasi, C., Good features to track. In: *IEEE Computer Vision and Pattern Recognition*, 593-600, 1994.
- [14] Rosten, E. and Drummond, T., Machine learning for high-speed corner detection. In: *European Conference on Computer Vision*, 430-443, 2006.
- [15] Lowe, D. G., Distinctive image features from scale-invariant keypoints. *International Journal of Computer Vision*, 60:91-110, 2004.
- [16] Bay, H., Ess, A., Tuytelaars, T., and Van Gool, L., Speeded-Up Robust Features (SURF). *Computer Vision and Image Understanding*, 110:346-359, 2008.
- [17] Viola, P. and Jones, M., Rapid object detection using a boosted cascade of simple features. In: *Proceedings of the IEEE Computer Society Conference on Computer Vision and Pattern Recognition*, 511-518, 2001.
- [18] Hartley, R. I. and Zisserman, A., *Multiple View Geometry in Computer Vision*, 2nd edition, Cambridge University Press, 2003.
- [19] Nyström, J., Oja, J., and Broman, N. O., Modelling the connection between industrially measured raw material properties and end user preferences. Part 1 - The simulation tool. In: *Proceedings of the IUFRO Working Party*, 2008.
- [20] Oja, J., Broman, N. O., and Nyström, J., Modelling the connection between industrially measured raw material properties and end user preferences. Part 3 - Optimizing the industrial production. In: *Proceedings of the IUFRO Working Party*, 2008.
- [21] Broman, N. O., Nyström, J., and Oja, J., Modelling the connection between industrially measured raw material properties and end user preferences. Part 2 - Results from preference studies. In: *Proceedings of the IUFRO Working Party*, 2008.
- [22] Bradski, G., The OpenCV Library. Dr. Dobb's Journal of Software Tools, 2000, <http://opencv-willowgarage.com>, last visited 2012-02-06.
- [23] Oyallon, E. and Rabin, J., SURF: Speeded-Up Robust Features, <http://www.ipol.im/pub/algo/or-speeded-up-robust-features/>, last visited 2012-02-07.
- [24] Fischler, M. A. and Bolles, R. C., Random Sample Consensus: A Paradigm for Model Fitting with Applications to Image Analysis and Automated Cartography. *Communications of the ACM*, 24:381-395, 1981.

---

---

# PAPER II

---

---

Recognition of boards using wood  
fingerprints based on a fusion of  
feature detection methods

**Authors:**

Tobias Pahlberg, Olle Hagman and Matthew Thurley

**Reformatted version of paper submitted to journal.**

© 2014, Tobias Pahlberg, Olle Hagman and Matthew Thurley



# Recognition of boards using wood fingerprints based on a fusion of feature detection methods

Tobias Pahlberg<sup>a,\*</sup>, Olle Hagman<sup>a</sup>, Matthew Thurley<sup>b</sup>

<sup>a</sup>Luleå University of Technology, Campus Skellefteå,  
Forskargatan 1, SE-931 87 Skellefteå, Sweden

<sup>b</sup>Luleå University of Technology,  
SE-971 87 Luleå, Sweden

## Abstract

This paper investigates the possibility to automatically match and recognize individual wooden boards using a fusion of two feature detection methods. The first method denoted *Block matching method*, detects corners and matches square regions around these corners using a normalized Sum of Squared Differences (SSD) measure. The second method denoted the *SURF* (Speeded-Up Robust Features) *matching method*, matches SURF features between images (Bay et al., 2008). The fusion of the two feature detection methods improved the recognition rate of wooden floorboards substantially compared to the individual methods. Perfect matching accuracy was obtained for board pieces with more than 20 knots using high quality images. More than 90% matching accuracy was achieved for board pieces with more than 10 knots, using both high- and low quality images.

**Keywords:** Wood fingerprint, Traceability, Feature detection, Biometrics, Hol-i-Wood Patching Robot

## 1. Introduction

The motivation for this work is: (i) to find out if it is possible for a machine vision system to correctly re-identify wooden boards using only their biometric “fingerprint”, and (ii) to find out exactly how small wood pieces can be recognized using a fusion of so called *feature detection* methods.

This is a continuation of the work done by Pahlberg and Hagman (2012) and is likewise a part of the *Hol-i-Wood Patching Robot* project. The project outcome will consist of several different *holonic* modules. Holonic, means that something is simultaneously a part of something whole, but can still work by itself, e.g., like a human cell. The wood fingerprint recognition system is such a part.

This particular application is supposed to run in real-time, meaning that the processing unit is only allowed a few hundredths of a second to correctly identify the wood piece when it arrives at one of the patching robots. The search space will consist of all the scanned wood

products that are, so to say, in the flow and on their way to being patched. This is therefore a so called *closed-set* identification task, where the sought “individual” is known to be in the database.

### 1.1. Traceability in the wood chain

The wood industry has been investigating solutions to a few traceability problems in the past. Efforts have been put into investigating the possibility of tracking trees between harvesting and sawmills using RFID tags (Björk et al., 2011; Häkli et al., 2013), tracking logs between the log sorting station and the saw intake (Chiorescu and Grönlund, 2004) and identifying which boards originate from which logs (Flodin et al., 2008). Attempts to recognize boards using board end images have also been carried out (Pölder et al., 2012). Other invasive technologies like barcode stickers and sprayed on paint have also been investigated (Dykstra et al., 2002).

One big gain with traceability of wood products would be the possibility for direct error feedback (Grönlund, 2008). If something is wrong with the end product, if it has the wrong moisture content, if the yield is low, there are possibilities to trace back through the chain and easier localize the origin of the problem.

\*Corresponding author. Address: Luleå University of Technology, Campus Skellefteå, Forskargatan 1, SE-931 87 Skellefteå, Sweden. Telephone: +46 (0)910-585336

Email address: tobias.pahlberg@ltu.se (Tobias Pahlberg)

Traceability would make it possible to do on-line and instantaneous calibration of machines. Today, time consuming and expensive test sawings are needed to calibrate machines and measurement equipment.

A wish, as expressed by industrial actors and researchers in the consortium WoodCentre North, is to generate a controlled flow for each individual wood component. This need is for example expressed by saw millers wanting to move away from bulk production to a more dynamic customer-ordered production process in order to utilize the biodiversity of wood better.

For the past decades, the trend has been to group similar logs into bins and sawing batches in the same way (Uusijärvi, 2000). However, in order for the wood industry to take the next step, there is a need to connect the information through the whole chain and adjust processing parameters by means of customer demands and optimizing for value.

Each log can be divided into several different products. Therefore, a high precision control is needed. The value added to each product, through different processing steps, will be lost if it ends up in the wrong bin. However, high precision control contradicts with keeping a low amount of equipment. It is much more effective to use in-process sensors as monitoring tools than adding new ones which are likely to not get the full service and care by the staff (Flodin, 2009).

A great advantage has emerged due to the possibility to look into the interior of logs with high precision at industrial speeds. The breakdown process can now be carried out virtually and a fingerprint extracted to later be recognized by a surface scanner.

Today, there are image sensors available in the process chain for sorting of logs by quality: 3D shape, discrete X-ray and computed tomography (CT). Surface scanners are present within green and dry sorting of the lumber and a number of process feedback sensors that can be utilized to track and control each individual product in the process. The sensors have different outputs and show different properties or mechanisms depending on sensor type. The problem which remains to be solved is to find appropriate fingerprint parameters and matching algorithms such that the wood products can be recognized at every point in the process.

Can this be done using sensors already present in the chain today, e.g., surface scanners? This article deals with the final stages of a wood value chain, i.e., so called tracking or re-identification of boards.

### 1.2. Biometrics

In the field of biometrics there has been an enormous amount of effort put in improving the recognition of hu-

mans (Jain and Kumar, 2012). A lot of different recognition techniques are today being researched in the field of biometric identification for security and prevention of identify theft (Komogortsev and Karpov, 2013; Yang et al., 2013; Czajka and Bulwan, 2013). As wood recognition and wood traceability are relatively unexplored areas of research there is a lot to learn from the human biometrics field. There, the most research and effort has up until today been put into fingerprint, face and iris recognition. However, there are also other applications, for example, palm print, vein, handwriting, sound, gait and ear recognition, that provide inspiration and push the biometrics field forward.

Luckily within wood fingerprint recognition we are spared from problems such as identify theft. However, some similar difficulties can still be present, as well as a few problems which are specific for the recognition of sawn wood products. Like humans, wood can age, which can lead to changes in color but also add crookedness, bow and cracks and so on (Sandberg, 2005). Wood products can also be dried, planed, sanded, treated by some reagent or cut into smaller pieces of different shapes during the processes within which we want to track it. In addition, measurements of wood in industrial processes can be subject to dirty, humid and other adverse environmental conditions. Things like sawdust or dirt, but also lighting can cause problems especially if we are using intensity information directly as feature representation.

The image acquisition can also be negatively affected by loss of traction of conveyor belts or improper clamping of the wood pieces in combination with line scan cameras.

Moreover, while there is a common saying that all trees are as unique as humans, there are also bound to be similar ones, that can cause problems. If thin veneer is cut from one log there will be several similar sheets, or "twins". The front and back of a board can also sometimes look very similar, though the sides will in that case be mirror images of each other.

### 1.3. Automatic fingerprint identification systems

Most often fingerprint identification systems, for humans or wood, need to address the following design steps (Jain et al., 1997):

1. Image acquisition
2. Fingerprint representation
3. Feature extraction
4. Matching

Systems usually use minutiae and their relative positions as fingerprint representation (Yager and Amin, 2004).

To be able to quickly match against very large databases, a great deal of care must be taken when choosing representation. Identification would often have to be made in haste since modern wood factories have very high flow speeds. For instance, modern sawmills run their conveyors at three meters per second.

Although speed is important in our real-time application, and though speed is always there in the back of our heads, it has not been top priority in this work. There are always strategies to speed up the final identification system. A more thorough optimization of the code will be done at a later stage, after proof of concept.

#### 1.4. Interest points and feature matching

*Interest points* are regions in an image that are likely to be recognized in other images of the same scene or object. Typical interest points include, for example, corners, line endings and blobs (Schmid et al., 2000). Corners, which are positions in an image where there is a strong intensity change in at least two directions, are very good objects to track (Moravec, 1980; Shi and Tomasi, 1994; Rosten and Drummond, 2006).

Usually, a representation of the intensity information in a region around the corner is stored. These feature representations, or *descriptors*, can later be used for recognition of objects by matching several feature descriptors between two images.

Criteria for good points to match were described by Förstner (1986) as having the following attributes:

1. *Distinctness*: The points should be distinguishable from their neighborhood, e.g., consist of a pronounced gradient in intensity or color.
2. *Invariance*: The points should be invariant with respect to expected geometric and radiometric distortions.
3. *Stability*: The points should be robust to noise.
4. *Seldomness*: There should not be several similar points in the same image to avoid confusion. (If a point is part of a repetitive pattern, the possibility for a false match is high.)
5. *Interpretability*: The points should preferably be interpretable, such as an edge, corner or blob.

Edges however, are usually not good interest points; the region information looks similar along the edge

and hence does not fulfill the seldomness requirement. Smooth untextured regions do not uphold the distinctness requirement.

There exists a lot of different feature detectors and descriptors. Some examples are: Scale-Invariant Feature Transform (SIFT, (Lowe, 2004)), Speeded-Up Robust Features (SURF, (Bay et al., 2008)), Gradient Location and Orientation Histogram (GLOH, (Mikolajczyk and Schmid, 2005)), Binary Robust Invariant Scalable Keypoints (BRISK, (Leutenegger et al., 2011)), Binary Robust Independent Elementary Features (BRIEF, (Calonder et al., 2010)), Oriented FAST and Rotated BRIEF (ORB, (Rublee et al., 2011)), Fast Retina Keypoint (FREAK, (Alahi et al., 2012)) and Principal Curvature-Based Regions (PCBR, (Deng et al., 2007)).

Each of them have their own strengths and weaknesses, and it is difficult to know beforehand which detector/descriptor combination will perform best for a certain dataset. Extensive evaluations of different detectors and descriptors have been carried out by Mikolajczyk and Schmid (2005) and Gauglitz et al. (2011). We decided to use two combinations of detectors and descriptors implemented in MATLAB R2011b since they are considered to be state-of-the-art methods and have been widely used in various tracking and object recognition systems (Gauglitz et al., 2011).

## 2. Material

To test a wood fingerprint recognition method, a large database and preferably also quite many query images, are needed. However, large image sets of board that have been scanned twice at moderately different settings, are not that common, unfortunately. Moreover, the two versions of the images may not be too similar and perfect, as this would render the problem quite trivial. Thus, the decision was made to re-scan a few available floorboards in lab environment.

In the near future, data will be collected from the scanner stations at the Hol-i-Wood Patching Robot plant.

### 2.1. Original dataset (database images)

The chosen dataset consists of 886 floorboard images from Scots pine (*Pinus sylvestris* L.) with the dimension 21x137 mm (Figure 1). The same dataset was previously used by Pahlberg and Hagman (2012) and the boards were originally scanned prior to a customer preference study in 2006 (Nyström et al., 2008; Broman et al., 2008; Oja et al., 2008).

The boards are between 3007-5109 mm long, with an average length of approximately 4500 mm. They were



Figure 1: Example of five boards from the original floorboard image dataset. The boards have been planed, sanded and finished with white pigmented oil. Their lengths have been cropped to 734 mm in this figure.

sawn from 222 logs with top diameter between 201-215 mm and were randomly collected from Bollsta sawmill in central Sweden. The boards were then planed, sanded and finished with white pigmented oil and a thin layer of varnish. The finished floorboards were scanned using a high resolution color line scan camera; Dalsa Trillium TR-37. It is a three-CCD camera with a 2048 pixel array for each of the colors; red, green and blue (Nyström et al., 2008). The boards were scanned at a resolution of 2.5 pixels/mm lengthwise and 10 pixels/mm across. Photocells were set up to automatically crop off 80 mm from each side to avoid edge artifacts. The images were then downsampled, using the function *imresize* in MATLAB, to a resolution of 1 pixel/mm in both dimensions using the *bicubic* interpolation setting and the default low-pass filter to mitigate aliasing. (Aliasing may appear as stair-step patterns at lines in an image or as Moiré patterns, a ripple- or wave-type artifact.)

Colors in the images were carefully calibrated to match the colors of the boards in reality. Then the im-

ages were saved in JPEG format at 95% quality.

## 2.2. Re-scanned dataset

The same line scan camera as before was used by Pahlberg and Hagman (2012) to re-scan 44/886  $\approx$  5% of the floorboards to have a subset of realistically acquired images to test the matching capabilities on. Some of the boards had during the past years of storage become somewhat crooked or bowed. Moreover, no stabilization of the boards was carried out this time while the conveyor belt was transporting them past the camera. No color corrections were made on the images and some dust stains were present on a few floorboards.

This time, the camera was mounted at such a distance from the conveyor belt that yielded a resolution of 5.6 pixels/mm lengthwise and 6.5 pixels/mm across. The entire lengths of the board images were kept this time, and the images were downsampled to 1 pixel/mm using the same method as before for consistency. They were saved in JPEG format at maximum quality.

## 2.3. Digital photos dataset (Canon)

Lower quality digital photos were taken of the same 44 floorboards from a distance to provide a tougher challenge for the recognition methods. The photos were acquired with a Canon 400D camera at a resolution of 0.6 pixels/mm. The images were upsampled to 1 pixel/mm in order not to disadvantage the scale-dependent block matching method. Scaling was again carried out using the bicubic interpolation setting. However, when upsampling images, no *a priori* low pass filtering is done.

## 2.4. Cropped image datasets

Many different subgroups of images were created from the 44 re-scanned boards and Canon digital photos. The images were cropped to shorter lengths so that each subgroup would contain board pieces with a specific number of knots, from 5, 6,  $\dots$ , 30 knots. The goal was to show how the different methods' performances vary with increased number of knots. Figure 2 shows examples of a wood piece from the group with five knots. A cropped version of the original dataset image is shown here as a reference, but when matching, the whole length of the original images were always used.

The amount of images in each group can be seen in Figure 3. Naturally, it was not possible to extract as many cropped images with a large amount of knots as with few knots, since in the latter case, several pieces could be grabbed from each board.





Figure 2: Examples of the cropped datasets with an approximate number of knots per image. Figures (a)-(c) are part of the 5-knot batch. Cropped versions of the original images are shown here as reference.

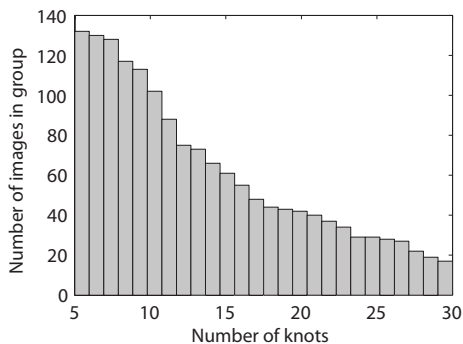


Figure 3: The amount of images in each group of the cropped datasets.

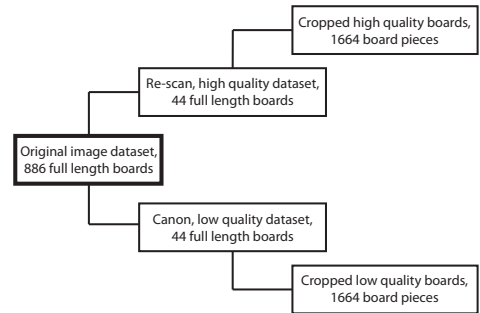


Figure 4: An overview of the different datasets used in this paper.

All knot positions (pixel coordinates) were marked manually in the computer to be able to determine good possible crop positions. A script was written to automatically cut the images in between knots. However, sometimes for Scots pine there are two or three knots at the same lengthwise position. This circumstance led to a few knots being cut in half. Nonetheless, the average number of knots in the images of each batch should be close to the target number.

Even very small knots were counted although they would probably not generate any stable interest points. However, very small knots on edges of the boards were not counted since features on edges of boards are removed in the matching algorithm. Some marginal differences in the crop positions between the high- and low quality dataset can occur, since the very smallest knots were not always visible in the low quality dataset, and was therefore not marked.

An overview of all different datasets can be found in Figure 4.

### 3. Methods

In this section the feature detection algorithms and the matching procedures are explained in order to be able to replicate the approach.

#### 3.1. Feature detection and matching

Two different feature detection methods were utilized individually, but also in combination, to carry out the identification of boards in the experiments. The first method will be referred to as the *Block matching method* (Nistér et al., 2004; MathWorks MATLAB; Szeliski, 2011, p. 222). The second method will be referred to as the *SURF matching method* (Speeded-Up Robust Features, (Bay et al., 2008)), and finally, the combination

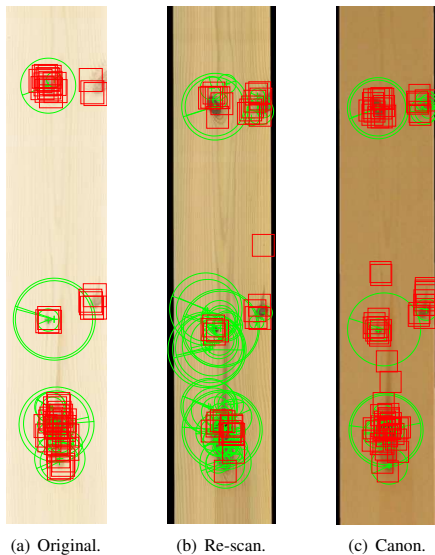


Figure 5: Examples of how the different features are being placed on the different datasets (same images as in Figure 2). Block features are shown with red squares and SURF features with green circles.

of the two will be denoted the *Fused method*. An example that illustrates how the feature descriptors are being placed on the different datasets can be seen in Figure 5.

The procedure for finding a best matching wood piece in the database is similar for the three methods. It can roughly be summarized as follows:

1. Load a query image.
2. Invoke a corner/blob detector on the image and extract features around those corners/blobs.
3. Remove features that are partly outside of the wood piece border.
4. Match query image features against database image features, one database image at a time (exhaustive search).
5. Estimate a best fitting geometric transformation between point matches.
6. Remove outlier matches that don't fit the transformation and evaluate if the transformation seems reasonable in terms of rotation and scaling.

The database image that has the most matching features is denoted the best match of the query. If two or

more database images get the same amount of matching features, no unique match was found and thus the wood piece could not be identified. However, this situation occurs quite seldom.

Two experiments were created to be able to answer the research questions stated in the beginning of the introduction.

- (i) Match the full length re-scanned images and also the Canon images against the original dataset.
- (ii) Match the cropped images in each group against the full length original images.

The matching accuracy is used to evaluate the results and is calculated as:

$$\frac{\text{Number of correct identifications}}{\text{Number of images in dataset, or group}} \cdot 100 (\%)$$

In this paper we only match images unrotated, or at least having very small rotation angles that were induced when scanning. The rotationally dependent Block matching method has been proven to work well for small rotations (Pahlberg and Hagman, 2012), but it cannot handle, for example, 180 degree rotations as it is now. Such added functionality would not be very difficult to implement but would increase the computation time.

Many components of the feature detection methods used in this paper can be found as open source implementations (Bradski, 2000), and they are often used for similar purposes in other computer vision applications.

In this paper, implementations from MATLAB<sup>®</sup> R2013a, Computer Vision System Toolbox<sup>™</sup> have been incorporated.

### 3.2. Block matching method

In the Block matching method the normalized intensity information in simple square neighborhoods are extracted as features around interest points in an image (Figure 6(a)). The block size extracted at every corner was set to  $25 \times 25$  pixels. This neighborhood size was chosen as a compromise between a large enough size to encircle substantial parts of the knots and a not too large size as to incur slow computation times. Relatively small regions also give us the possibility to extract features close to wood piece edges, as features lying directly on an edge are rejected. A detailed explanation of the procedure is given in Algorithm 1.

Interest points were obtained using Harris corner detector (Harris and Stephens, 1988) as opposed to our previous work (Pahlberg and Hagman, 2012), where

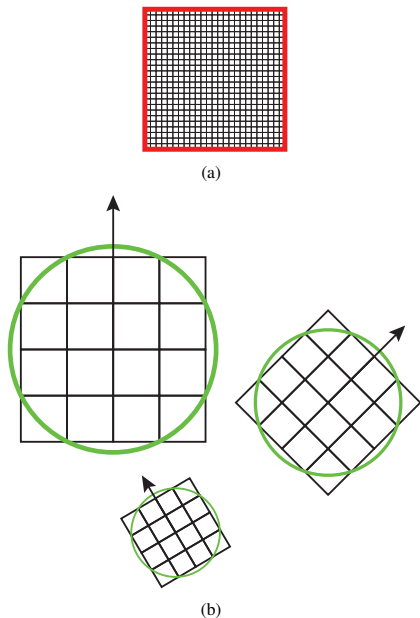


Figure 6: (a) A simple  $25 \times 25$  Block feature. (b) Three SURF features of different sizes and orientations. The interest points' dominant directions are marked by the arrows.

the FAST corner detector was used (Rosten and Drummond, 2006). The FAST corner detector was found to return too much false corners along jagged lines; hence a switch of corner detector was made. A Gaussian filter of size  $5 \times 5$  pixels and  $\sigma = 5/3$  is used as part of the Harris corner detector to smooth gradients and reduce noise before the actual corner extraction in all dataset images. The threshold for accepting corners is set as a fraction of the maximum corner metric value in that image. This fraction was lowered to 0.005 instead of the default value 0.01 in order to retrieve more corners. However, no limit was set on the amount of corners to be returned.

For comparing blocks, normalized Sum of Squared Differences (SSD) was chosen as metric. A threshold for rejecting matches is specified as a percentage of the worst case scenario for the SSD between two normalized vectors. This percentage is then converted to a numeric value between the best case and the worst case; on the interval  $[0, 4]$ . The threshold for rejecting matching blocks was increased from 1% to 2% ( $\Rightarrow 0.02 \cdot 4$ ) to approve more matches than the default.

The MATLAB-function *matchFeatures* carries out

the matching procedure. The function takes two sets of features, matches these and returns a list of indices connecting the features that match.

### 3.3. SURF matching method

Speeded-up Robust Features (SURF) are robust scale- and rotationally invariant features which are fast to compute and suitable for object detection and recognition. This feature detector was chosen because of its popularity and since it was readily available.

The features are made invariant to rotation by aligning them along the dominant direction of the interest point within a circular neighborhood (Figure 6(b)). (However, in this study, the scale- and rotational invariance does not come into play, since all images are of roughly of the same scale and rotation.)

SURF uses *integral images* (Viola and Jones, 2001) for fast calculations of sums of intensities over square regions in grayscale images. The use of integral images makes it possible to do such computations in constant time, independent of region size. In the SURF approach, the kernel sizes are resized instead of the images, which otherwise has been the common way to create scale spaces in the past. The SURF descriptor is a  $16 \times 4 = 64$ D-vector, representing normalized gradient statistics (mean and absolute mean values) extracted from a spatial grid divided into 4-by-4 cells (Oyallon and Rabin, 2013).

SURF is thoroughly described in Bay et al. (2008), and an extensive algorithm description can be found in Oyallon and Rabin (2013). A condensed version is presented here in Algorithm 2.

The settings used for SURF in our implementation is given in Table 1. These settings will extract descriptors that have a size of between  $9 \times 9$ , and up to  $147 \times 147$  pixels (or mm) in the images. The threshold for accepting interest points was lowered substantially compared to our previous work (Pahlberg and Hagman, 2012).

The SSD percentage threshold is also in this method converted to a numerical value ( $5\% \Rightarrow 0.05 \cdot 4$ ).

The MATLAB-function *matchFeatures* carries out the matching procedure of the SURF algorithm.

Table 1: Settings for SURF in our implementation

Parameter	Our value	Default
Scale-space octaves	3	3
Scale levels within octaves	6	4
Thresh. to accept features	150	1000
Max no. of SURF features	$\infty$	$\infty$
SSD thresh. to accept match	5%	1%

**Algorithm 1** Block matching method

- 1: Invoke Harris corner detector on query image,  $I_A$ , and database image,  $I_B$ .
- 2: Extract the intensity information in a square patch around the corners.
- 3: Patches that are on the border or completely outside the region of interest are removed.
- 4: Reshape the patches into  $n_A$  and  $n_B$  column vectors and insert them as the columns of feature matrices  $A$  and  $B$ .
- 5: Normalize the columns of  $A$  and  $B$  to make the method more robust to radiometric differences.
- 6: Calculate the  $(n_A \times n_B)$  score matrix between all the features in  $A$  and  $B$  using SSD according to:

$$\text{score}(i, j) = \sum (\mathbf{a}_i - \mathbf{b}_j)^2,$$

where  $\mathbf{a}_i$  and  $\mathbf{b}_j$  are the column vectors of  $A$  and  $B$  respectively, and the operator  $(\cdot)^2$  squares every element in a vector.

- 7: **for** every row in *score* **do**
- 8:     Find the indices  $(r, c)$  of the lowest score, i.e., the best matching feature between  $I_A$  and  $I_B$ .
- 9:     Remove query feature  $r$  and database feature  $c$  from the score matrix by setting the corresponding score values to  $\infty$ .
- 10: **end for**

**Algorithm 2** SURF matching method

- 1: Create a scale-space representation of the query image and the database image by use of integral images and box filters.
- 2: Use the local maxima of the Hessian determinant operator applied to the scale-space to obtain interest points (blobs).
- 3: Keep points with a response level above a certain threshold.
- 4: Refine scale and location of these candidates.
- 5: SURF points which are on the border or completely outside the region of interest are removed.
- 6: Calculate a dominant orientation direction using the neighborhood gradient information to make the feature descriptors rotationally invariant.
- 7: Build a 64-dimensional descriptor corresponding to the local normalized gradient histograms using Haar wavelets.
- 8: Calculate the  $(n_A \times n_B)$  score matrix between all the features in  $A$  and  $B$  using SSD, as in Algorithm 1.
- 9: **for** every row in *score* **do**
- 10:     Find the indices  $(r, c)$  of the lowest score, i.e., the best matching feature between  $I_A$  and  $I_B$ .
- 11:     Remove query feature  $r$  and database feature  $c$  from the score matrix by setting the corresponding score values to  $\infty$ .
- 12: **end for**

## 3.4. Removing false matches

Some features of wood, such as knots, can look quite similar, especially to a computer that hasn't been trained properly or using enough parameters. Knots are usually somewhat circular and similar in size and color. Usually there will be a few very similar looking knots on a board. This leads to the possibility that a feature in one image can be matched to several features in another image. To take care of this problem, the method *NearestNeighborSymmetric* was chosen in MATLAB for matching both Block- and SURF-features. This method only returns unique matches in addition to using the match threshold. A feature vector is matched to its nearest neighbor in the other feature set, and for a match to be accepted, both points must be the best matching feature of the other (side symmetry).

MATLAB's Geometric Transform Estimator (GTE) was utilized to exclude outlier matches given a best fitting geometric transformation between the locations of the interest points. The computationally simple *non-reflective similarity* transformation was chosen since we are dealing with small and simple geometric distortions.

The similarity transformation consists of an isotropic scaling, a rotation and a translation (Hartley and Zisserman, 2003). This means that the shapes of the objects are preserved which is a reasonable approximation for an application with wooden boards if the cameras are set up properly.

The Euclidean pixel distance threshold was set to 100 to allow for some deviation from the exact transformation, mainly to handle warp of the boards. Random Sample Consensus, (RANSAC, (Fischler and Bolles, 1981)), was chosen as the method for determining inlier matches. The GTE with RANSAC iteratively picks a few matched point pairs, estimates a transformation, and checks how many inliers are within a threshold. The transform with most inliers is chosen as the correct one and the inliers are the accepted matches.

A problem may arise where many features in a tight cluster in one image are sometimes matched to scattered points in the other image (Figure 7(a)). This problem was taken care of by investigating the transformation,  $T$ , returned by the GTE. If the similarity transformation led to a scaling of more than 5%, or if the rotation angle

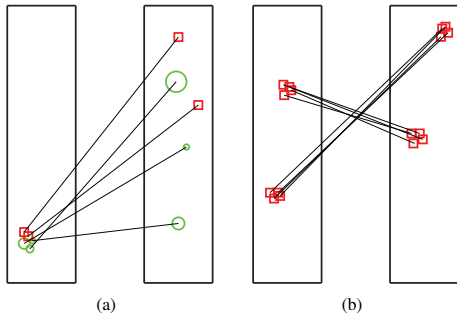


Figure 7: Two of the most common types of false matches. (a) A tight cluster of features falsely matched to sparsely scattered features. (b) Highly ambiguous features that are falsely matched.

Table 2: Matching accuracy in % using entire board images as queries.

Dataset	Block	SURF	Fused
Re-scanned	93.1	97.7	100.0
Canon	93.0	81.4	97.7

was more than 5 degrees, the “hit” would be discarded.

If four or more features were found within a 3 cm radius, the cluster of features was discarded altogether as the features were decided to be too ambiguous, see example in Figure 7(b).

## 4. Results

### 4.1. Matching full length boards

When the entire board images were used as queries, all 44 boards were found using the Fused method for the high resolution dataset (Table 2). The Block matching method has similar performance for both datasets in this test. The SURF method performs somewhat better on the higher resolution dataset.

Matching of whole boards was also done in our previous work (Pahlberg and Hagman, 2012). Compared to the previous results, the switch to Harris corner detector for the Block matching method dramatically increased the matching accuracy on the low resolution Canon dataset, from 9.1% to 93.0%. For the high resolution dataset, the accuracy decreased slightly, from 95.5% to 93.1%.

The lowered threshold for accepting interest points for the SURF method increased the recognition accuracy from 34.1% to 81.4% on the low quality dataset. For the high quality dataset, the accuracy was increased from 86.4% to 97.7%.

Through screening tests it was found that the thresholds for accepting interest points affected the matching accuracy the most. In Tables 3-6, the impact of the new threshold choices can be seen compared to the default values, and what impact this change has on for example inlier percentage, execution time and matching accuracy.

Notable from these tables is that the matching accuracy is high even when the inlier percentage is quite low. This fact highlights the importance of the geometric transform estimator.

### 4.2. Matching cropped images

An example of two successfully matched cropped images can be seen in Figure 8(a)-(b), for the high quality and the low quality dataset respectively.

In Figure 9(a)-(b) the matching accuracy is plotted against the number of knots of each group. The accuracy increases quite rapidly with increasing number of knots for all methods and both datasets. For all methods the increase in matching accuracy starts to slow down between 10-15 knots.

The fusion of the two methods performs best and reaches 100% matching accuracy for board pieces with more than 20 knots for both datasets. For the low quality dataset, the matching accuracy seemingly drops a little when boards contain more knots. This drop was caused by one of the boards, where the majority of the features were falsely matched.

The SURF matching method performs better on the high resolution dataset than on the low resolution counterpart for any amount of knots. The SURF method and the Block method have similar performance on the high resolution dataset independent of the amount of knots.

Most often, the Block method extracts a more features per query image compared to the SURF method using the settings specified in Section 3.2 and 3.3. Therefore, when a correct matching board is found, usually the Block method has the most matching features.

Both methods extract more than double the amount of features from the high resolution dataset compared to the low resolution.

Noteworthy is that the simple Block matching method has a substantially higher performance on the lower resolution, blurry, digital photos compared to the SURF matching method. The Block method also performs much better on the low resolution images than on the higher resolution images between 5-15 knots. Between 15-30 knots, there is no distinguishable performance difference between the datasets for the Block method.

Table 3: Block matching statistics (Re-scan dataset) on the 44 full-length boards while changing corner threshold. Median values are shown for # inliers, # interest points and execution time.

Corner threshold	# inliers	# interest points	% inliers	Exec. time (s)	Matching acc. (%)
0.01 (default)	16	87	18	18	91
0.005 (new)	22	148	15	28	93

Table 4: Block matching statistics (Canon dataset) on the 44 full-length boards while changing corner threshold. Median values are shown for # inliers, # interest points and execution time.

Corner threshold	# inliers	# interest points	% inliers	Exec. time (s)	Matching acc. (%)
0.01 (default)	11	46	24	13	84
0.005 (new)	17	66	26	17	93

Table 5: SURF method statistics (Re-scan dataset) on the 44 full-length boards while changing blob threshold. Median values are shown for # inliers, # interest points and execution time.

Blob threshold	# inliers	# interest points	% inliers	Exec. time (s)	Matching acc. (%)
1000 (default)	10	44	23	10	93
150 (new)	15	170	9	15	98

Table 6: SURF method statistics (Canon dataset) on the 44 full-length boards while changing blob threshold. Median values are shown for # inliers, # interest points and execution time.

Blob threshold	# inliers	# interest points	% inliers	Exec. time (s)	Matching acc. (%)
1000 (default)	6	28	21	10	67
150 (new)	6	45	13	11	81

## 5. Discussion

There are a lot of parameters that can be tweaked to calibrate and improve performance of identification systems that utilize feature detectors. The sensitivity of the interest point detectors and the thresholds to accept point matches are the most obvious. One improvement would be to implement a smarter approach for accepting interest points. In the Block matching method, the Harris corner acceptance threshold is adaptive and depends on the highest corner response value in that image. This is not appropriate if one corner value is much higher than the others. It can lead to less distinct knots not being found. Another solution would be to detect a certain number of corners, for example, the 300 strongest corners. This solution would also make it possible to have control over the computation time. The optimal window size for the corner/blob detector, together with the appropriate amount of *a priori* smoothing of the image, must also be investigated.

The fusion of the two methods performs best, which was expected. Therefore, we recommend a combination of different feature detectors as they complement each other and react to different positions in an image. More extracted features in general seem to increase the chances of finding the right wood piece but at the ex-

pense of computation time. As can be noted in Figure 8(b), the SURF method had only one matching feature in this particular case. A solution could be to lower the threshold for accepting blobs, or to change the algorithm to allow feature descriptors to have more than one match each.

The simple Block matching method showed a surprisingly high performance for the lower resolution, blurry, digital photos. This implies that *a priori* blurring of the query images could possibly increase the performance of the Block method. The reason why the SURF method performs worse on this dataset is because its blob detector does not extract as many, or as well spread out, interest points as the Harris corner detector. Often Harris corner detector finds many different corners around each knot, as opposed to the SURF method’s Fast-Hessian based blob detector which often only finds 1-2 points. The SURF method’s blob detector extracts more interest points on the high resolution dataset, where it reacts to places even on clearwood. The scale- and rotational invariance of SURF should not yield any special advantage nor disadvantage, since both query and database images were approximately unrotated and of the same scale.

The quality of the input images certainly has an im-

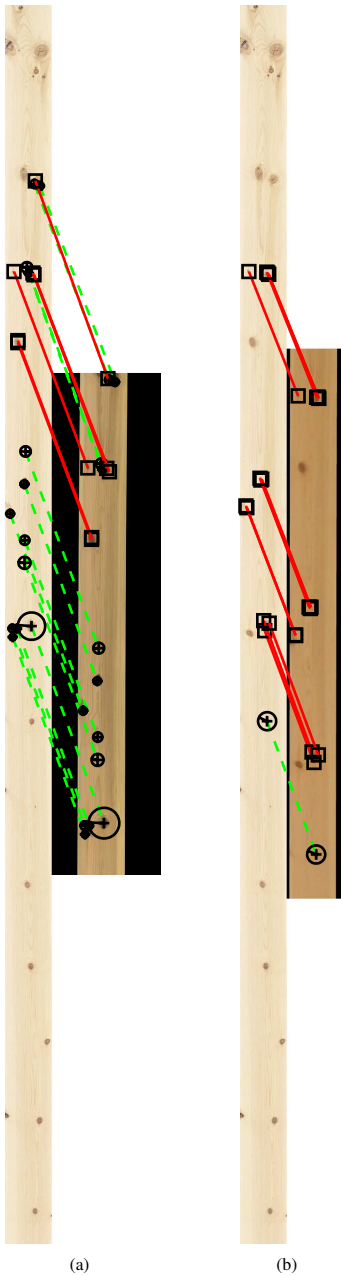
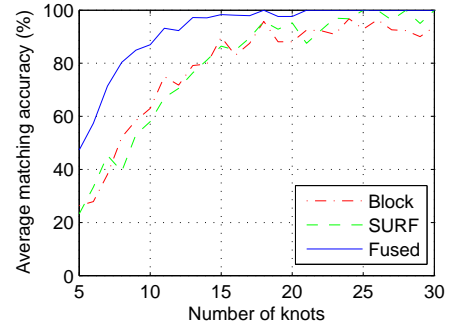
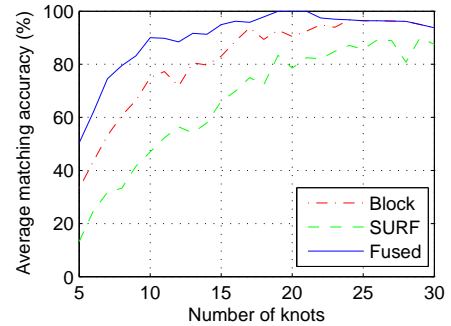


Figure 8: Two successful matchings from the cropped image group with eight knots using the Fused method. (a) Re-scanned dataset. (b) Canon dataset.



(a)



(b)

Figure 9: (a) Matching accuracy of subsets of the Re-scanned floorboards. (b) Matching accuracy of subsets of the digital photos.

impact on the recognition accuracy. The smoothness of the board surfaces would also affect the result. However, preliminary tests have shown that rough sawn surfaces yield more interest points than smooth surfaces, like on our floorboards. This fact should translate to better recognition possibilities for roughly sawn products. The staining with white pigmented oil used in this study should not give any special advantage or disadvantage since the feature descriptors normalize the intensity within each feature descriptor region.

In this work, all possible solutions were always tested in a “brute-force” manor, meaning a complexity of  $O(n)$ . To increase speed, the search space could be reduced by grouping similar wood fingerprints into bins or by sorting similar ones after some measure. Measures such as for example the variance of colors of the boards or the average distance between knots, could be used. Moreover, parallelization could be implemented, utilizing multi-core processors or graphic cards, as a lot of

the computations are independent of each other.

## 6. Conclusions

- The fusion of the *Block matching method* and the *SURF method* improved the recognition rate of wooden boards substantially over the individual feature detection methods.
- Approximately 100% matching accuracy was obtained on our material for board pieces with more than 20 knots using both high- and low quality images.
- More than 90% matching accuracy was achieved for board pieces with more than 10 knots, using both high- and low quality images.
- The individual feature detection methods extract much more features from high quality images than from those of low quality.
- The recognition rate could be increased for boards with few knots by extracting more interest points, but at the expense of longer computation time.

## 7. Future work

Future work will include investigation of how knot positions and other geometric relationships between knots could be utilized for recognition. Moreover, there is a need to further investigate which corner/blob detectors and feature descriptors are the most suitable for different kinds of wood surfaces and given different types of noise.

## Acknowledgements

This work has been part of the Hol-i-Wood Patching Robot project and received funding from the European Union's Seventh Framework Programme (FP7/2007-2013) under grant agreement no. 284573. The Hol-i-Wood PR is a collaboration between Luleå University of Technology (LTU), TU Wien and TU München, as well as industrial partners; MiCROTEC, Springer, TT-Tech and LIP-BLED.

## References

Alahi, A., Ortiz, R., Vandergheynst, P., 2012. FREAK: Fast Retina Keypoint, in: IEEE Conference on Computer Vision and Pattern Recognition, Ieee, New York. CVPR 2012 Open Source Award Winner.

- Bay, H., Ess, A., Tuytelaars, T., Van Gool, L., 2008. Speeded-Up Robust Features (SURF). *Computer Vision and Image Understanding* 110, 346–359.
- Björk, A., Erlandsson, M., Häkli, J., Jaakkola, K., Nilsson, Å., Nummilla, K., Puntanen, V., Sirkka, A., 2011. Monitoring environmental performance of the forestry supply chain using RFID. *Computers in Industry* 62, 830 – 841.
- Bradski, G., 2000. The OpenCV Library. *Dr. Dobb's Journal of Software Tools*.
- Broman, N.O., Nyström, J., Oja, J., 2008. Modelling the connection between industrially measured raw material properties and end user preferences. Part 2 - Results from preference studies, in: Proceedings of the IUFRO Working Party 5.01.04. Joensuu, Finland.
- Calonder, M., Lepetit, V., Strecha, C., Fua, P., 2010. Brief: Binary robust independent elementary features, in: Proceedings of the 11th European Conference on Computer Vision: Part IV, Springer-Verlag, Berlin, Heidelberg. pp. 778–792.
- Chiorescu, S., Grönlund, A., 2004. The fingerprint method: Using over-bark and under-bark log measurement data generated by three-dimensional log scanners in combination with radiofrequency identification tags to achieve traceability in the log yard at the sawmill. *Scandinavian Journal of Forest Research* 19, 374–383.
- Czajka, A., Bulwan, P., 2013. Biometric verification based on hand thermal images, in: Biometrics (ICB), 2013 International Conference on, pp. 1–6.
- Deng, H., Zhang, W., Mortensen, E., Dietterich, T., Shapiro, L., 2007. Principal Curvature-Based region detector for object recognition, in: 2007 IEEE Conference on Computer Vision and Pattern Recognition, IEEE. pp. 1–8.
- Dykstra, D.P., Kuru, G., Taylor, R., Nussbaum, R., Magrath, W.B., Story, J., 2002. Technologies for Wood Tracking, In: Environmental and Social Development East Asia and Pacific Region Discussion Paper. Technical Report. World Bank.
- Fischler, M.A., Bolles, R.C., 1981. Random sample consensus: A paradigm for model fitting with applications to image analysis and automated cartography. *Comm ACM* 24, 381–395.
- Flodin, J., 2009. KAP - Kontinuerlig Automatisk Provsågning. Technical Report. WoodCenter North.
- Flodin, J., Oja, J., Grönlund, A., 2008. Fingerprint traceability of sawn products using industrial measurement systems for x-ray log scanning and sawn timber surface scanning. *Forest Products Journal* 58, 100 – 105.
- Förstner, W., 1986. A feature based correspondence algorithm for image matching. *International Archives of Photogrammetry, Remote Sensing, and Spatial Information Sciences* 26, 150–166. Rovaniemi.
- Gauglitz, S., Höllner, T., Turk, M., 2011. Evaluation of interest point detectors and feature descriptors for visual tracking. *Int. J. Comput. Vision* 94, 335–360.
- Grönlund, A., 2008. SkeWood - Ett forskningsprogram vid Luleå tekniska universitet. Technical Report 25. LTU Skellefteå.
- Häkli, J., Sirkka, A., Jaakkola, K., Puntanen, V., Nummilla, K., 2013. Challenges and Possibilities of RFID in the Forest Industry, Radio Frequency Identification from System to Applications, Dr. M. I. B. Reaz (Ed.). InTech. chapter 15. pp. 301–324.
- Harris, C., Stephens, M., 1988. A Combined Corner and Edge Detection, in: Proceedings of The Fourth Alvey Vision Conference, pp. 147–151.
- Hartley, R.I., Zisserman, A., 2003. Multiple View Geometry in Computer Vision. 2nd ed., Cambridge University Press, ISBN: 0521540518.
- Jain, A., Hong, L., Pankanti, S., Bolle, R., 1997. An identity-authentication system using fingerprints. *Proceedings of the IEEE* 85, 1365–1388.



- Jain, A.K., Kumar, A., 2012. Biometric recognition: An overview, in: Mordini, E., Tzovaras, D. (Eds.), *Second Generation Biometrics: The Ethical, Legal and Social Context*. Springer Netherlands, volume 11 of *The International Library of Ethics, Law and Technology*, pp. 49–79.
- Komogortsev, O.V., Karpov, A., 2013. Liveness detection via oculomotor plant characteristics: Attack of mechanical replicas, in: 2013 International Conference on Biometrics (ICB), pp. 1–8.
- Leutenegger, S., Chli, M., Siegwart, R.Y., 2011. Brisk: Binary robust invariant scalable keypoints, in: *Proceedings of the 2011 International Conference on Computer Vision*, IEEE Computer Society, Washington, DC, USA, pp. 2548–2555.
- Lowe, D.G., 2004. Distinctive image features from scale-invariant keypoints. *International Journal of Computer Vision* 60, 91–110.
- MathWorks MATLAB, 2013. *Computer Vision System Toolbox: 2013b - Video Stabilization Using Point Feature Matching*. The MathWorks Inc., Natick, Massachusetts, United States.
- Mikolajczyk, K., Schmid, C., 2005. A performance evaluation of local descriptors. *IEEE Transactions on Pattern Analysis & Machine Intelligence* 27, 1615–1630.
- Moravec, H., 1980. *Obstacle Avoidance and Navigation in the Real World by a Seeing Robot Rover*. Technical Report CMU-RI-TR-80-03.
- Nistér, D., Naroditsky, O., Bergen, J., 2004. Visual odometry, in: *IEEE conference on computer vision and pattern recognition (CVPR'04)*, pp. 652–659.
- Nyström, J., Oja, J., Broman, N.O., 2008. Modelling the connection between industrially measured raw material properties and end user preferences. Part 1 - The simulation tool, in: *Proceedings of the IUFRO Working Party 5.01.04*, Joensuu, Finland.
- Oja, J., Broman, N.O., Nyström, J., 2008. Modelling the connection between industrially measured raw material properties and end user preferences. Part 3 - Optimizing the industrial production, in: *Proceedings of the IUFRO Working Party 5.01.04*, Joensuu, Finland.
- Oyallon, E., Rabin, J., 2013. An analysis and implementation of the SURF method, and its comparison to SIFT. <http://www.ipol.im/pub/pre/69/preprint.pdf>, last visited 2014-04-06.
- Pahlberg, T., Hagman, O., 2012. Feature recognition and fingerprint sensing for guiding a wood patching robot, in: Quenneville, P. (Ed.), *World Conference on Timber Engineering*, pp. 724–733.
- Pölder, A., Juurma, M., Tamre, M., 2012. Wood products automatic identification based on fingerprint method. *Journal of Vibroengineering* 14.
- Rosten, E., Drummond, T., 2006. Machine learning for high-speed corner detection, in: *European Conference on Computer Vision*, pp. 430–443.
- Rublee, E., Rabaud, V., Konolige, K., Bradski, G.R., 2011. Orb: An efficient alternative to sift or surf., in: Metaxas, D.N., Quan, L., Sanfeliu, A., Gool, L.J.V. (Eds.), *ICCV, IEEE*. pp. 2564–2571.
- Sandberg, D., 2005. Distortion and visible crack formation in green and seasoned timber: influence of annual ring orientation in the cross section. *Holz als Roh- und Werkstoff* 63, 11–18.
- Schmid, C., Mohr, R., Bauckhage, C., 2000. Evaluation of interest point detectors. *International Journal of Computer Vision* 37, 151–172.
- Shi, J., Tomasi, C., 1994. Good features to track, in: *Computer Vision and Pattern Recognition, 1994. Proceedings CVPR '94*, 1994 IEEE Computer Society Conference on, pp. 593–600.
- Szeliski, R., 2011. *Computer Vision: Algorithms and Applications*. Springer London.
- Uusijärvi, R., 2000. *Automatic tracking of wood*. Ph.D. thesis. Kungliga Tekniska Högskolan. Institutionen för produktionssystem.
- Viola, P., Jones, M., 2001. Rapid object detection using a boosted cascade of simple features, in: *Computer Vision and Pattern Recognition, 2001. CVPR 2001. Proceedings of the 2001 IEEE Computer Society Conference on*, pp. 1–511 – 1–518 vol.1.
- Yager, N., Amin, A., 2004. Fingerprint classification: a review. *Pattern Analysis & Applications* 7, 77–93.
- Yang, J., Lei, Z., Liao, S., Li, S.Z., 2013. Face liveness detection with component dependent descriptor, in: *2013 International Conference on Biometrics (ICB)*, pp. 1–6.



---

---

# PAPER III

---

---

Wood fingerprint recognition using  
knot neighborhood  $K$ -plet  
descriptors

**Authors:**

Tobias Pahlberg, Erik Johansson, Olle Hagman and Matthew Thurley

**Reformatted version of paper submitted to journal.**

© 2014, Tobias Pahlberg, Erik Johansson, Olle Hagman and Matthew Thurley



---

## Wood fingerprint recognition using knot neighborhood $K$ -plet descriptors

Tobias Pahlberg · Erik Johansson · Olle Hagman ·  
Matthew Thurley

**Abstract** In the wood industry there is a need to recognize and track wood products through a production chain. This would facilitate improved process control and extraction of quality measures of various production steps. In this paper, a novel wood surface recognition system that uses scale- and rotationally invariant features descriptors called  $K$ -plets is described and evaluated. The idea behind these descriptors is to use information of how knots are positioned in relation to each other. The performance and robustness of the proposed system is tested on images of 212 wood panels with varying levels of normally distributed errors applied to the knot positions. The results showed that the proposed method is able to successfully identify 99-100% of all panel images with knot positional error levels that can be expected in practical applications.

**Keywords** Wood fingerprint,  $K$ -plet, recognition, neighborhood descriptor, Hol-i-Wood PR

### 1 Introduction

The motivation behind this work comes from companies wanting to recognize and track solid wood products through their production chain. The recognition method should not interfere with, or have a negative effect on the existing processes. The method should preferably utilize sensors already available in the production chain and not introduce new ones. Today, recognition and tracking tasks are often carried out by aid of barcode labels or paint (Uusijärvi, 2000, p. 64-73, Dykstra et al., 2002; Flodin, 2009).

This work is part of the EU project *Hol-i-Wood Patching Robot*, where one task is to recognize shuttering panels at an automatic patching station. The project will in the end have resulted in a completely automatized patching system which will be placed at the wood products producer LIP-BLED in Slovenia.

Tracking capabilities of wood pieces in a non-invasive way requires a method to assign *wood fingerprints* to every “individual”. A fingerprint should include properties such that it becomes

---

Tobias Pahlberg  
Luleå University of Technology, Forskargatan 1, 93187, Skellefteå, Sweden  
Tel.: +46-910-585336  
E-mail: tobias.pahlberg@ltu.se

Erik Johansson  
Luleå University of Technology, Forskargatan 1, 93187, Skellefteå, Sweden  
SP Technical Research Institute of Sweden, Laboratorgränd 2, 93177 Skellefteå, Sweden  
Tel.: +46-10-5166278  
E-mail: erik.johansson@ltu.se

possible to identify a unique wood piece. Visually salient features, geometric features or material properties are examples which can be utilized for this purpose.

The two most common, distinct, visual features on sawn lumber are usually knots and growth ring patterns. The presence of visual features in the images, of course, highly depends on wood species, sawing method and image acquiring technique.

A robust matching method that does not rely on the wood piece keeping its exact shape is desirable since it will increase the number of possible applications. Wood products are often cut or milled into smaller pieces in industrial processes. In these cases it would not be possible to directly use knot coordinates as measures of the positions of the features. However, the intrinsic geometrical relations between knots may be used instead.

In many applications it is also advantageous if the recognition method can handle the case when an object appears at a different rotation or in a different scale. It might be difficult in reality to obtain the exact same camera setup and conditions in two places. In some cases it might not even be possible, or desirable, to have two similar camera setups due to high costs, space or flow speed.

The objective of this study is to evaluate the performance and robustness of a novel matching algorithm for wooden panels. The proposed algorithm uses a feature descriptor called *K-plets*, originally proposed by Chikkerur et al. (2005) to encode the local neighborhoods of human fingerprint features called *minutiae*. Our paper was inspired by this original work, but here the *K-plets* are based upon knots and their relative positions. Using knot patterns when identifying wood surfaces has not been done in previous studies. The proposed algorithm is not affected by different scales or rotations of the panel images, i.e., it is scale- and rotationally invariant. However, it is sensitive to other anisotropic geometric distortions. This approach would in a real-world application require a method for segmenting knots from clearwood. Since knot segmentation is well established in the literature (Åstrand, 1996; Funck et al., 2003; Todoroki et al., 2010), it is outside the scope of this article. Instead, the effects of the precision of knot detection and segmentation are evaluated.

## 2 Related work

### 2.1 Point pattern matching

Points or regions in an image, which have a high probability of being detected even after geometric and radiometric distortions have been applied to the image, are usually referred to as *feature points*. Feature points could be, for example, distinctive blobs, corners or other high curvature points. If this is applied to wood, feature points could for example be knots, resin pockets and certain annual ring patterns. Except for naturally occurring features on wood surfaces, there may also be other features induced by handling, such as dirt or dents. *Point pattern matching* is a problem that consists of finding correct point matches between two images or scenes (Chang et al., 1997). This problem has previously been addressed in, for example, star and constellation recognition (Spratling and Mortari, 2009), biometrics (Jain et al., 2007, Chap. 1-2), image stitching (Brown and Lowe, 2007) and 3D point cloud registration (Gruen and Akca, 2005).

According to Chang et al. (1997) there are a few problems associated with point pattern matching in general:

1. The images of the objects to be recognized can have been acquired using different camera setups and at different times. Hence, the objects can have different rotation, scale or position.
2. Due to radiometric differences and dissimilar noise conditions there may be inaccuracies introduced in the positions of the extracted feature points.
3. One of the point sets might only be a subset of the other. Noisy images might have both removed feature points and introduced false ones.
4. Point pattern problems often involve huge datasets which leads to a necessity for a fast and effective matching strategy.

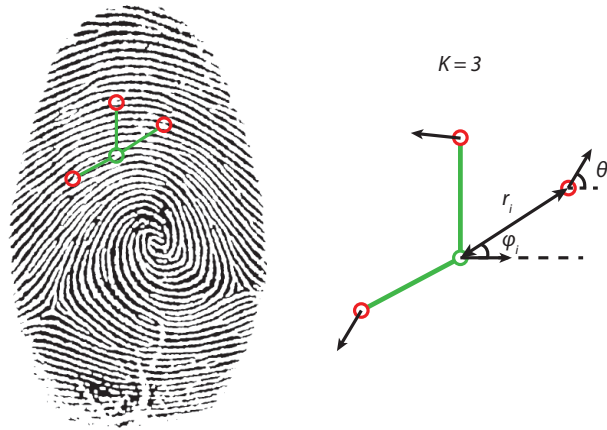


**Fig. 1** The original  $K$ -plet representation. Here,  $(r_i, \varphi_i)$  is the polar coordinate of neighbor  $i$  with respect to the central minutia,  $m_c$ .  $\theta_i$  is the relative angle of neighbor  $i$  with respect to  $m_c$ . (Illustration inspired by Chikkerur et al. (2005))

Although this paper focuses on point pattern matching, there are other related techniques to match sets of points to each other. A common example is the 3D shape matching algorithm *Iterative Closest Point* (ICP) proposed by Besl and McKay (1992) and Chen and Medioni (1992).

## 2.2 $K$ -plet representation

This article presents a feature point neighborhood representation called  $K$ -plets, which was originally proposed as a fingerprint descriptor by Chikkerur et al. (2005). The original paper's nomenclature is presented here as an introduction to the subject.

A  $K$ -plet describes the geometry of a local neighborhood around a certain fingerprint minutia (Figure 1). It consists of a central minutia,  $m_c$ , and  $K$  neighboring minutiae  $\{m_1, m_2, \dots, m_K\}$ . Each neighborhood minutia is described by its distance,  $r$ , to the central minutia, the angle,  $\varphi$ , of the line connecting the central minutia and the neighbor and the relative orientation of the neighboring minutiae compared to that of the central minutia,  $\theta$ .

Complete rotational invariance is obtained by rotating the  $K$ -plet to align with the direction of the central minutia,  $\theta_c$ , with the  $x$ -axis.

The neighbors of each  $K$ -plet are put in a sequence ordered by increasing number of radial distance. Later, the matching is carried out by comparing two ordered sequences using a string alignment algorithm. This type of matching strategy handles the possible problem of one or a few missing or added neighborhood minutiae in each  $K$ -plet. However, this added functionality of handling missing features increases the complexity and therefore computation time of the matching step.

## 2.3 Segmenting knots from images of wood

Knot positions are the main input for the fingerprint descriptor that is proposed in this paper. Segmentation of knots from wood panel images is thus important when identifying fingerprints.



Fig. 2 Example of a few boards from the floorboard dataset put next to each other.

Totally automatic and robust knot segmentation is challenging to achieve using only RGB-images. It can be quite difficult to divide knots and background (clearwood) into two classes since knots can have exactly the same color and brightness as clearwood. Growth rings, reaction wood, pith and other defects can further complicate the thresholding task. However, much work has been done in the field of automatic segmentation of knots on board images (Åstrand, 1996; Funck et al., 2003; Todoroki et al., 2010). Modern wood surface scanners often deal with the problem by utilizing both X-ray and the *tracheid effect* to more accurately detect knots (GoldenEye; WoodEye).

### 3 Material and methods

This section describes how the dataset of panel images that were used for performance tests were created and how the knot positions were extracted. After that, the  $K$ -plet descriptors are explained and how they were adapted to work on the panel dataset. Lastly, the descriptor matching procedure is presented and how the performance tests were carried out.

#### 3.1 Creating a dataset

A total of 212 simulated panel images were constructed by stitching together board images from an available floorboard dataset. The simulated panel dimensions were chosen to be similar to the formwork panels produced by an industrial partner of the European research project Hol-i-Wood PR. This means panels of 3000 mm length and four boards ( $4 \times 137$  mm = 548 mm) of width.

The floorboard dataset consists of 886 floorboard images from Scots pine (*Pinus sylvestris* L.) with the dimension  $21 \times 137$  mm (Figure 2) and were originally scanned for a customer preference study (Broman et al., 2008; Nyström et al., 2008; Oja et al., 2008). These boards were sawn from 222 logs with top diameter between 201-215 mm which were randomly collected from Bollsta sawmill in central Sweden.

#### 3.2 Extraction of knot positions

The aim of extracting knot positions from the panel dataset was to obtain a database of realistic knot distributions on panels. With such data, the accuracy of the proposed neighborhood descriptors ( $K$ -plets) could be tested. For the tests to be relevant, it was not necessary to extract the exact knot positions from the panel dataset as long as the knot distributions were realistic.



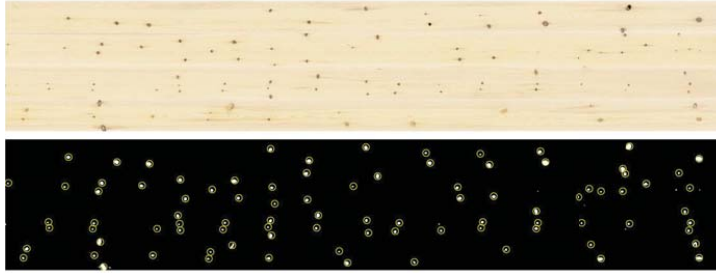


Fig. 3 Floorboard panel and thresholded image of the same panel.

To extract knot distributions, a semi-automatic approach was adopted. First, an automatic segmentation of knots was made as described in the list below, and then the segmented image and knot centroids were displayed on screen as seen in Figure 3. If the positions were deemed approximately correct by manual inspection, the centroid positions,  $(x, y)$ , were saved. The exact rejection criteria in the manual inspection are not crucial for this study; it suffices to say that outliers were removed in this step. Below follows a detailed description of the knot centroid extraction procedure, which was conducted in MATLAB:

1. Pick 4 board images from the dataset. Crop the board images to 3000 mm length, stitch them together to a panel and convert it to grayscale.
2. Smooth the image using a  $5 \times 5$  mm averaging filter to suppress growth rings.
3. Perform an edge detection with a morphological black top-hat filtering (rolling ball filter) using a circular structuring element with radius 12 mm. Knots are accentuated by this procedure while regions of compression wood, which have similar appearance as uneven lighting, are suppressed. The transformation of image  $I$  is defined as:  $T_{SE}(I) = I \bullet SE - I$ , where  $\bullet$  is a closing operation and  $SE$  is a grayscale structuring element.
4. Threshold the resulting image into two classes using Otsu's method (Otsu, 1979). (The method tries to separate an image into two classes, black and white, while minimizing the intra-class variance.)
5. Fill holes in the logical image,  $BW$ , using the MATLAB command: `imfill(BW, 'holes')`. This function performs hole filling by morphological reconstruction (Gonzalez and Woods, 2008, p. 660).
6. Remove small or thin regions in the image by aid of the MATLAB function `regionprops` (MathWorks MATLAB, a). A region is considered small or thin if the area is less than  $36 \text{ mm}^2$  or the eccentricity is higher than 0.98. These values were chosen since a majority of such regions in the logical images were unlikely to be knots. This fact was observed by manual inspection.

### 3.3 Neighborhood descriptors ( $K$ -plets)

The  $K$ -plet neighborhood descriptor in our implementation is similar to the one used by Chikkerur et al. (2005). An exception is that there is no orientation included for our minutiae, i.e., knots. This parameter has been neglected in this work to keep a low computational complexity and to lower the requirements of a knot segmentation algorithm.

After a knot detection algorithm has obtained the centroids of the knots on a wood piece, the problem boils down to matching points between images.  $K$ -plets describe local geometric relationships between points and can thus also be used for wood fingerprint recognition.

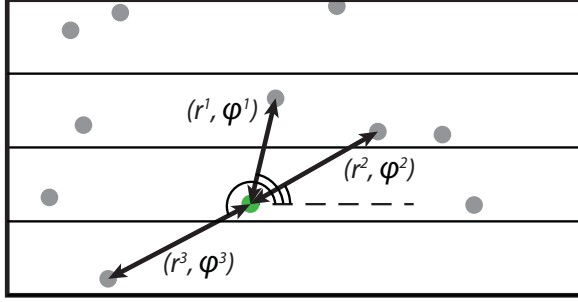


**Fig. 4** The neighborhood descriptor for  $K = 3$  visualized on a surface with gray circles representing knots. Each of the  $K$  neighboring knots has a distance  $r^j$  at an angle  $\varphi^j$  to the center knot.

The distances and angles from every knot to  $K$  neighboring knots were picked as descriptors of knot neighborhoods. See Figure 4 for an example using three knot neighbors.

The neighborhood  $K$ -plets' distances and angles for one panel can be stored as rows in a matrix for each wood piece according to:

$$P = \begin{bmatrix} r_1^1 & r_1^2 & \dots & r_1^K & \varphi_1^1 & \varphi_1^2 & \dots & \varphi_1^K \\ r_2^1 & r_2^2 & \dots & r_2^K & \varphi_2^1 & \varphi_2^2 & \dots & \varphi_2^K \\ \vdots & \vdots & & \vdots & \vdots & \vdots & & \vdots \\ r_m^1 & r_m^2 & \dots & r_m^K & \varphi_m^1 & \varphi_m^2 & \dots & \varphi_m^K \end{bmatrix}, \quad (1)$$

where the neighbors are sorted with ascending value of  $r$ , i.e.,  $r_i^1$ , and  $\varphi_i^1$  correspond to the closest neighbor to knot  $i$ .  $m$  is both the number of knots and number of  $K$ -plets on the panel.

### 3.3.1 Scale- and rotational invariance

Scale- and rotational invariance is obtained by computing ratios between the radial distances and differences between the angles within each  $K$ -plet. The matrix  $P$  in Equation 1 is modified as

$$P^* = \begin{bmatrix} r_1^{(2/1)} & r_1^{(3/1)} & \dots & r_1^{(K/1)} & \varphi_1^{(2-1)} & \varphi_1^{(3-1)} & \dots & \varphi_1^{(K-1)} \\ r_2^{(2/1)} & r_2^{(3/1)} & \dots & r_2^{(K/1)} & \varphi_2^{(2-1)} & \varphi_2^{(3-1)} & \dots & \varphi_2^{(K-1)} \\ \vdots & \vdots & & \vdots & \vdots & \vdots & & \vdots \\ r_m^{(2/1)} & r_m^{(3/1)} & \dots & r_m^{(K/1)} & \varphi_m^{(2-1)} & \varphi_m^{(3-1)} & \dots & \varphi_m^{(K-1)} \end{bmatrix}, \quad (2)$$

where  $P^*$  is of size  $m \times (2K - 2)$  and each row corresponds to a  $K$ -plet. In the matrix,  $r_i^{(j/1)} = r_i^j / r_i^1$  and  $\varphi_i^{(j-1)} \in [0, \pi]$  is the closest angle between knots  $j$  and 1 for the  $i$ :th  $K$ -plet.

### 3.3.2 Normalization of descriptor data

The  $K$ -plet column values need to be normalized in order for all distance ratios and angles to have the same weight in the identification. All  $P^*$  matrices for the query and database panels were normalized column-wise according to

$$P^* \rightarrow \left[ \frac{P_1^* - \mu_1}{\sigma_1}, \frac{P_2^* - \mu_2}{\sigma_2}, \dots, \frac{P_{2K-2}^* - \mu_{2K-2}}{\sigma_{2K-2}} \right], \quad (3)$$

where  $P_i^*$  is a column vector of length  $m$ .  $\mu_i$  and  $\sigma_i$  are the mean and standard deviation of  $P_i^*$ .

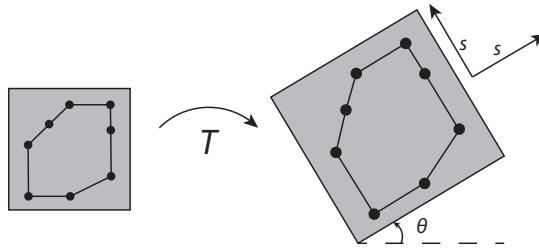


Fig. 5 The similarity transformation,  $T$ , where  $\theta$  is the rotation and  $s$  is an isotropic scale factor.

### 3.4 Matching of descriptors

To identify a query panel in a database of panels, the  $K$ -plets of the query panel are compared to the  $K$ -plets of each database panel. The best matching database panel is obtained by counting the number of matching  $K$ -plets,  $N$ , for each database panel and evaluating which panel gave the highest value. To illustrate this procedure, we will describe how  $N$  is calculated when matching  $K$ -plets from a query panel,  $Q$ , to those of a specific panel in the database,  $D$ . This calculation is done in two steps, where the first is to obtain a set of probable matches, and the second is to refine that selection by removing erroneous matches.

#### 3.4.1 Sum of squared differences

The quality of the match between two  $K$ -plets is calculated as the sum of squared differences (SSD) of the elements (squared Euclidean distance). A perfect match will have an SSD of 0, while a bad match will have a relatively high SSD. The SSD is calculated for all possible  $K$ -plet pairs between  $Q$  and  $D$ . All matches that have an  $SSD < \lambda$  are extracted and subject to further processing as described in Section 3.4.2. We denote this set of matching  $K$ -plets as  $A$ . The optimal threshold,  $\lambda$ , for our dataset was computed in the matching performance test.

#### 3.4.2 Removal of erroneous matches

MATLAB's geometric transform estimator (GTE) was utilized on the centroids of the matching  $K$ -plet pairs in  $A$  to remove outlier matches and thus improving the panel matching accuracy. The number of inliers,  $N$ , after applying the GTE was used as a measure of how well a database panel matches a query panel. The best matching panel in the database was the one with the highest value of  $N$ .

The GTE uses Random Sample Consensus (RANSAC, (Fischler and Bolles, 1981)) to enable completion of the estimation within a given time frame. We assume only simple geometric differences between query and database panel images, i.e., a similarity transformation consisting of rotation, scale and translation as seen in Figure 5. The GTE will iterate and randomly select, in this case, two centroid pairs to compute a transformation matrix that best fits the input points. The success of estimating a correct geometric transform using RANSAC heavily depends on the percentage of correctly matched point pairs given as input (MathWorks MATLAB, b). To obtain good results, the percentage of inliers should be kept at the highest level possible. A reasonable inlier percentage is obtained by choosing a suitable  $\lambda$ -threshold. Another way to improve the panel recognition rate is to increase the number of random samplings (iterations). Herein lies a trade-off between better results and computation time. The settings for the GTE were in this study chosen as in Table 1.

**Table 1** Settings for the geometric transform estimator used in our tests.

Parameter	Setting
Method	'Random Sample Consensus (RANSAC)'
ExcludeOutliers	true
Transform	'Nonreflective similarity'
PixelDistanceThreshold	100
NumRandomSamplings	1000

### 3.5 Matching performance test

It is important to test how the knot detection precision affects the panel recognition rate, since the proposed matching algorithm relies upon knot centroids. To test this, we simulated three error levels when detecting knot centroid positions. These errors were normally distributed with zero mean and standard deviations of  $\sigma_\epsilon = [5, 8, 11]$  mm. Positional error was measured in Euclidean distance.

In addition to errors in position, a portion of all knots in the panels were randomly removed,  $p_\epsilon = [0, 5, 10, 15]$  %. With three error levels in knot position and four distinct knot removal portions, a total of  $3 \times 4 = 12$  cases were studied. For each of the 12 cases, a panel database of  $K$ -plets,  $D_{\sigma,p}$ , with a specific error level was created. A total of 3 query datasets of  $K$ -plets,  $Q_\sigma$ , were created where each corresponded to a knot positional error level.

The matching tests were conducted so that each query dataset was matched to each of the four databases with the same error level in knot position as the query dataset. For example, query dataset  $Q_5$  was matched to each of the four databases  $\{D_{5,0}, D_{5,5}, D_{5,10}, D_{5,15}\}$ . The accuracy was calculated as the percentage of correctly matched panels. Thus, 12 accuracy values were calculated, where each represents a specific error level.

To get a better understanding of the impact of the value  $K$ , several  $K$ -values were evaluated:  $K \in \{4, 6, 8, 10\}$ . The previously described procedure of validation was used on each choice of  $K$ -values.

The mean computational time of matching one query panel to a database panel was calculated. This was done in MATLAB R2013b by measuring the time the matching algorithm needed to match all 212 query panels to all 212 database panels twelve times (once for each error level). In other words, this means a total of  $212 \times 212 \times 12$  times. The measurement was done with the  $K$  and  $\lambda$ -value which gave the best accuracy. A laptop of model HP EliteBook 8560w with Intel Core i7-2670QM processor at 2.20 GHz, 64-bit Windows 7 operating system and 8.00 GB RAM was used.

## 4 Results

The results of the matching accuracy tests described in Section 3.5 are shown in Figure 6. From that figure, it is clear that  $K = 6$  is the optimal value in this study. To obtain an accuracy of at least 99% with  $K = 6$ , the positional error standard deviation must not exceed 5 mm whilst detecting at least 85% of the knots. If all knots can be successfully detected, then the knot positional error is allowed to be 8 mm. Detailed results with  $K = 6$  are shown in Table 2. The results in this table highlight the importance of maintaining a low knot positional error.

The SSD threshold for accepting possible matches was set to  $\lambda = 1.4$ . That specific threshold was chosen since it resulted in the best overall performance of the algorithm. However, our tests showed that the performance of the algorithm was quite stable even when changing the parameter  $\lambda$ .

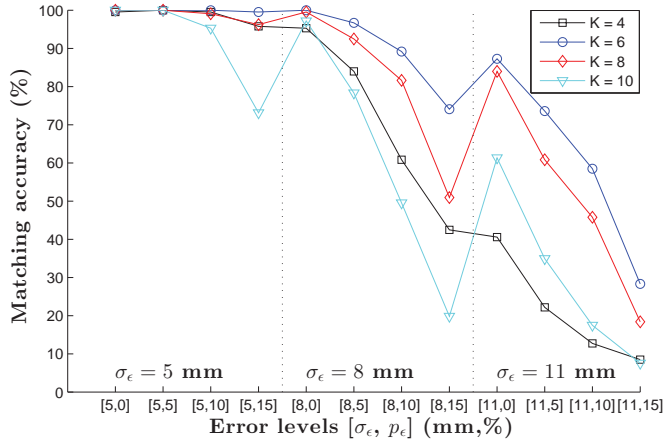


Fig. 6 The matching accuracy for different values of  $K$  and error levels.

When using  $K = 6$  and  $\lambda = 1.4$ , the tests of computational time showed that the average time of matching two panels to each other was 3.65 ms. If the database would contain 1000 panels, the average computational time for matching a query panel to such a database would be 3.65 s using the same hardware setup and MATLAB implementation.

Table 2 Accuracy of the matching algorithm with  $K = 6$  and  $\lambda = 1.4$ .

Accuracy (%)	100	100	100	99.5	100	96.7	89.2	74.1	87.3	73.6	58.5	28.3
Positional error (mm)	5	5	5	5	8	8	8	8	11	11	11	11
Removed knots (%)	0	5	10	15	0	5	10	15	0	5	10	15

## 5 Discussion

The proposed method using  $K$ -plet descriptors, SSD matcher and geometrical transform estimator, is scale- and rotationally invariant. This fact renders the method useful in more than just panel matching with well-defined orientation and scale. For example, if a piece of wood is divided into several smaller objects, the smaller parts can be matched to the piece they originated from. This requires that the pieces contain enough knots to be well defined with  $K$ -plets.

For matching algorithms to be used in practice they need high enough matching accuracy. The necessary accuracy depends on the application and in our specific case of matching panels it should be higher than 99%. Our results show that this is possible with the proposed method if the error in knot position has a standard deviation of 5 mm or less. It is important for the accuracy that the knot segmentation is consistent on both the database image and the corresponding query image. The image acquisition needs to be similar enough so that the image quality does not affect the knot segmentation. Aside from errors related to knot segmentation, the accuracy is affected by the size

of the database and the frequency of knots. A smaller database would likely increase the accuracy since it would decrease the search space in the matching step. This would also reduce the total computational time which increases linearly with database size. The panels used in this study had a relatively high number of knots, but if the algorithm is used on panels with just a handful of knots, it would likely be rather inaccurate. How many knots that are needed has not been investigated and such a threshold is difficult to guess. However, there is no reason to expect that the algorithm would not work if only half the amount of knots were available compared to the panels used in this study.

Funck et al. (2003) evaluated several wood defect detection algorithms on color images of Douglas fir (*Pseudotsuga menziesii* (Mirb.) Franco) veneer sheets. The color images used in that study had a resolution of 1.7 mm/pixel compared to our color images with 1 mm/pixel. In their tests, many of the algorithms had a mean error of less than 5 mm when calculating knot centroid position. This indicates that our proposed feature matching algorithm is feasible for industrial applications. However, in the current study, the panels used were constructed from boards which are cut in a different way than veneer sheets. Knot shape is approximately circular on veneer sheets, but on boards they have more diverse shapes which makes knots more difficult to segment. The results from Funck et al. (2003) still give an indication of the expected accuracy in knot position measurements on wooden boards. Knot segmentation algorithms are therefore likely sufficiently accurate for applications using our matching algorithm.

## 6 Conclusions

- This paper presents a scale- and rotationally invariant algorithm for matching wooden panels. This method opens up possibilities for a broad range of applications.
- The proposed algorithm uses a novel approach based on internal knot structure. For the Scots pine panels used in this study, the algorithm was successful, as should be the case for panels of other wood species that contain a similar frequency of knots.
- Our algorithm uses knot positions; consequently the segmentation accuracy is very important. According to previous publications on knot segmentation, the proposed matching algorithm should be good enough for industrial applications.

## 7 Future work

There are several ways to improve our algorithm further. In this paper, the  $K$ -plets consist of knot centroids, but they could also incorporate knot shape and type, as well as size and orientation relative to the other knots in the  $K$ -plet. This adds other requirements to a knot segmentation algorithm, but with extra information it is reasonable to expect that the requirements of knot centroid precision would decrease.

**Acknowledgements** This work has been part of the Hol-i-Wood Patching Robot project and received funding from the European Union's Seventh Framework Programme (FP7/2007-2013) under grant agreement no. 284573. The Hol-i-Wood PR is a collaboration between Luleå University of Technology (LTU), TU Wien and TU München, as well as industrial partners; MiCROTEC, Springer, TTTech and LIP-BLED.

## References

- Åstrand, E., 1996. Automatic Inspection of Sawn Wood. Linköping Studies in Science and Technology, Linköping University.

- Besl, P.J., McKay, N.D., 1992. A method for registration of 3-d shapes. *IEEE T Pattern Anal* 14, 239–256.
- Broman, N.O., Nyström, J., Oja, J., 2008. Modelling the connection between industrially measured raw material properties and end user preferences. Part 2 - Results from preference studies, in: *Proceedings of the IUFRO Working Party 5.01.04, Joensuu, Finland*.
- Brown, M., Lowe, D.G., 2007. Automatic panoramic image stitching using invariant features. *Int. J. Comput. Vision* 74, 59–73.
- Chang, S.H., Cheng, F.H., Hsu, W.H., Wu, G.Z., 1997. Fast algorithm for point pattern matching: Invariant to translations, rotations and scale changes. *Pattern Recognition* 30, 311 – 320.
- Chen, Y., Medioni, G., 1992. Object modelling by registration of multiple range images. *Image Vision Comput.* 10, 145–155.
- Chikkerur, S., Cartwright, A., Govindaraju, V., 2005. K-plet and coupled bfs: A graph based fingerprint representation and matching algorithm, in: Zhang, D., Jain, A. (Eds.), *Advances in Biometrics*. Springer Berlin Heidelberg, volume 3832 of *Lecture Notes in Computer Science*, pp. 309–315.
- Dykstra, D.P., Kuru, G., Taylor, R., Nussbaum, R., Magrath, W.B., Story, J., 2002. Technologies for Wood Tracking, In: *Environmental and Social Development East Asia and Pacific Region Discussion Paper*. Technical Report. World Bank.
- Fischler, M.A., Bolles, R.C., 1981. Random sample consensus: A paradigm for model fitting with applications to image analysis and automated cartography. *Comm ACM* 24, 381–395.
- Flodin, J., 2009. KAP - Kontinuerlig Automatisk Provsågning. Technical Report. WoodCenter North. In Swedish.
- Funck, J., Zhong, Y., Butler, D., Brunner, C., Forrer, J., 2003. Image segmentation algorithms applied to wood defect detection. *Computers and Electronics in Agriculture* 41, 157 – 179.
- GoldenEye, . Microtec GmbH, <http://www.microtec.eu>.
- Gonzalez, R., Woods, R., 2008. *Digital Image Processing (3rd Edition)*. Pearson Prentice Hall.
- Gruen, A., Akca, D., 2005. Least squares 3d surface and curve matching. *ISPRS J Photogramm* 59, 151 – 174.
- Jain, A.K., Flynn, P., Ross, A.A., 2007. *Handbook of Biometrics*. Springer-Verlag New York, Inc., Secaucus, NJ, USA.
- MathWorks MATLAB, 2013a. *Image Processing Toolbox: 2013b*, The MathWorks Inc., Natick, Massachusetts, United States.
- MathWorks MATLAB, 2013b. *Computer Vision System Toolbox: 2013b*, The MathWorks Inc., Natick, Massachusetts, United States.
- Nyström, J., Oja, J., Broman, N.O., 2008. Modelling the connection between industrially measured raw material properties and end user preferences. Part 1 - The simulation tool, in: *Proceedings of the IUFRO Working Party 5.01.04, Joensuu, Finland*.
- Oja, J., Broman, N.O., Nyström, J., 2008. Modelling the connection between industrially measured raw material properties and end user preferences. Part 3 - Optimizing the industrial production, in: *Proceedings of the IUFRO Working Party 5.01.04, Joensuu, Finland*.
- Otsu, N., 1979. A Threshold Selection Method from Gray-level Histograms. *IEEE Transactions on Systems, Man and Cybernetics* 9, 62–66.
- Spratling, B.B., Mortari, D., 2009. A survey on star identification algorithms. *Algorithms* 2, 93–107.
- Todoroki, C., Lowell, E., Dykstra, D., 2010. Automated knot detection with visual post-processing of douglas-fir veneer images. *Computers and Electronics in Agriculture* 70, 163 – 171.
- Uusjärvi, R., 2000. Automatic tracking of wood. Ph.D. thesis. Kungliga Tekniska Högskolan. Institutionen för produktionssystem.
- WoodEye, . Innovativ Vision AB, <http://www.woodeye.se>.







